CHAPTER 7 RESULTS AND DISCUSSION

Diffusion of silver into single crystalline 6H-SiC was investigated using the two methods discussed in Chapter 5. With first method surface layer diffusion was examined. For this a silver layer was deposited onto clean single crystal 6H-SiC samples. These were then annealed under vacuum to temperatures below the melting point of silver. The results of the post annealing Rutherford backscattering spectroscopy (RBS) and SEM analyses indicated no in-diffusion of silver and an absence of silver on and in the SiC at these temperatures. This was hypothesized to be the result of a wetting problem between silver and SiC. Further, the layer in-diffusion of silver was investigated by encapsulation. SiC samples were encapsulated in a quartz ampoule together with a silver source to maintain a silver vapour layer on the samples' surface during annealing. The encapsulated samples were annealed at temperatures below the quartz softening temperature (1200 ^{o}C). The post annealing RBS and SEM analyses results indicated no in-diffusion of silver into 6H-SiC and an absence of silver on 6H-SiC surfaces.

Due to the negative results of the layer in-diffusion of silver into 6H-SiC, further research was undertaken into silver diffusion in 6H-SiC by ion implantation. Silver was implanted in 6H-SiC at different temperatures (i.e. room temperature (23 ^{o}C), 350 ^{o}C and 600 ^{o}C) at a fluence of 2×10^{16} cm^{-2}. The samples were then annealed from 700 ^{o}C up to 1600 ^{o}C for different annealing times. Using RBS the silver depth profiles after implantation and after annealing were compared to calculate diffusion coefficients. RBS-C was employed to investigate the production of radiation damage and also the annealing out of radiation damage during annealing. SEM was utilised to investigate the changes occurring on the sample surfaces during annealing.

This chapter presents and discusses the results of this study and is organised as follows: section 7.1 discusses the layer in-diffusion results and 7.2 the implantation results.

7.1 LAYER IN-DIFFUSION

The in-diffusion of a vacuum deposited layer of naturally-occurring silver into 6H-SiC was investigated using RBS and SEM at temperatures below the melting point of silver (T_m= 960 ^oC). Due to the extremely low diffusion in this temperature range [Jia04], samples with silver deposited on their surfaces had to be kept in the vacuum furnace for very long periods (100 hours or more). Even then a direct determination of the silver diffusion profile near the surface was not guaranteed. Therefore, silver was to be chemically removed after annealing so as to analyse the exposed SiC surface for any penetration of silver, exploiting the higher depth resolution resulting from the much reduced energy straggling from the top surface silver layer.

The samples were then annealed at 800 ^oC for 10 hours, which is a temperature well below the melting point of silver (960 ^oC). The RBS and SEM analyses indicated that the deposited silver disappeared without diffusing into SiC. At first we believed this was due to the sublimation of silver at that temperature. However, the vapour pressure calculation at 1000 ^oC in Appendix A does not confirm our initial belief.

Owing to this problem, the samples with 100 nm of silver on their surface were vacuum encapsulated together with a silver source in a quartz ampoule, as explained in chapter 5. The purpose of the said source was to maintain a silver layer or silver vapour on the samples' surface. The encapsulated samples were thereafter annealed in a vacuum at 800 ^oC, 900 ^oC and 1000 ^oC for 10 h. The RBS analyses of the annealed samples indicated that no silver was left on the surfaces and also discovered no trace of diffused silver beyond the silicon carbide surfaces. These results were confirmed by SEM in conjunction with EDS. However, silver was found on the walls of the quartz glass ampoule. At first we thought this to be supporting the suggestion of the sublimation of silver. No further annealing was performed at temperatures above 1000 ^oC to avoid the softening of quartz glass, which at occurs around 1200 ^oC.

The disappearance of the silver layer from the SiC surface was investigated further at temperatures from 200 ^oC to 700 ^oC. This was undertaken by isochronal annealing

(for 30 minutes) at temperatures from 200 ^{o}C to 700 ^{o}C. The SEM results depicted in Figure 7-1 show that the as-deposited silver layer is fairly smooth and possesses a homogenous structure. Silver islands start to form at 200 ^{o}C and become larger and more visible as the annealing temperature increases up to 400 ^{o}C. At the lower temperatures (200 to 400 ^{o}C), facet formation indicates the polycrystalline nature of these islands which is clearly visible in the SEM images. At the higher temperatures these long facets islands break into bigger and smaller facets islands. This is due to the coalescence of the smaller islands into bigger islands along with increasing drop formation. The black spots in the SEM image of the sample annealed at 200 ^{o}C are cavities (indicated by C) in the Ag layer. Defects in the Ag layer, such as grain boundaries, internal stresses, and local weak bonding between Ag and SiC, could trigger cavity formation. In the same SEM image the straight lines inside the large crystals could be micro twins, indicated by T. Some of the larger silver islands also exhibit grain grooving or steps on the surface. The islands that are formed at higher temperatures, e.g. at 700 ^{o}C, are composed of small islands clustered together and bigger islands with openings between them - see the low magnification image in figure 7-1 (the un-labelled image).

The formation of islands is the result of weaker binding forces between silver atoms and SiC as compared to the binding forces between silver atoms and such islands constitute the proof that silver does not wet SiC. Therefore, the disappearance of silver is caused by the formation of silver islands on the SiC surface and their coalescence into droplets, which run off the samples' surface in longer duration annealing.

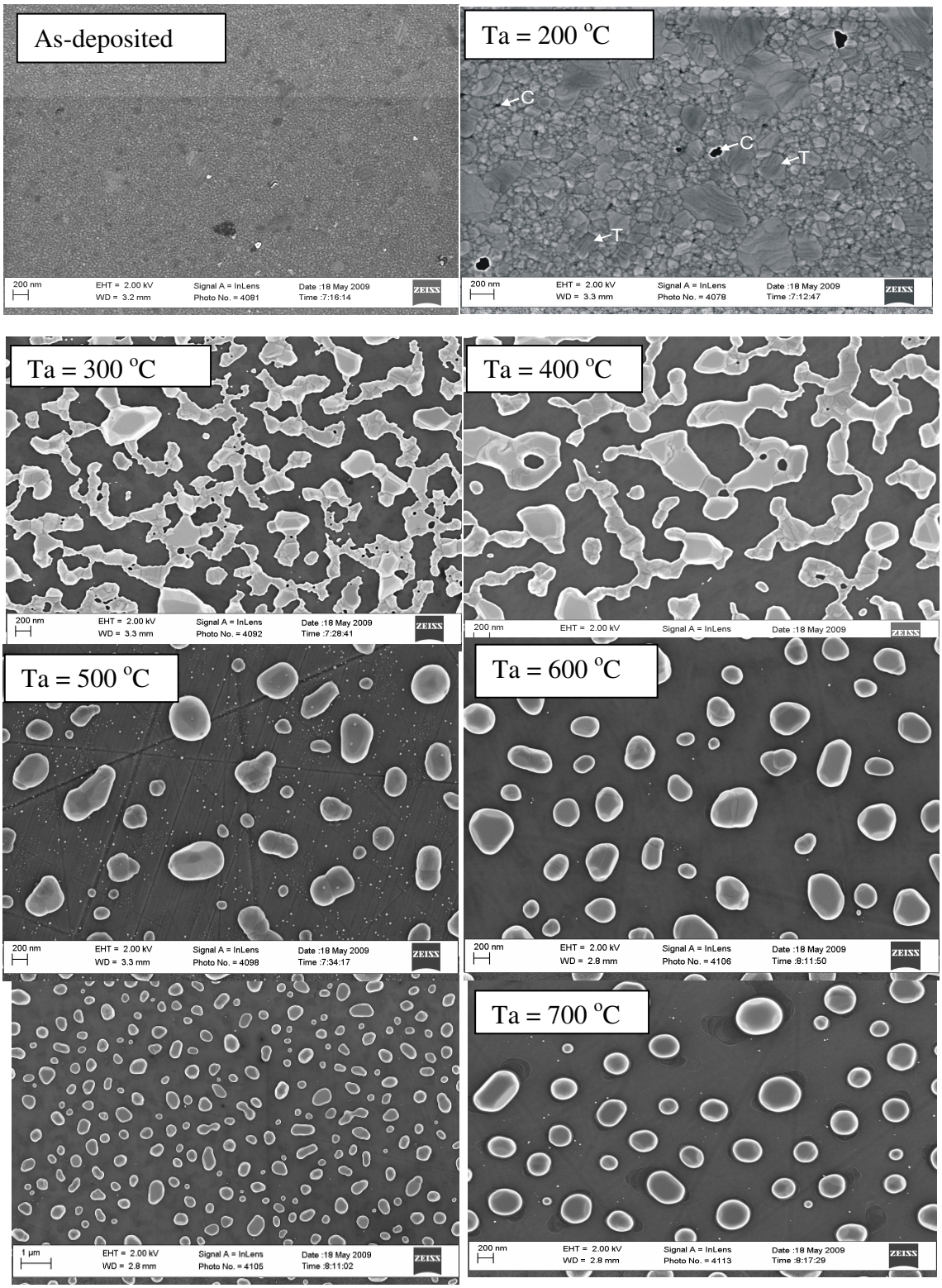

Figure 7-1: SEM images of a 100 nm silver layer vacuum deposited on 6H-SiC after isochronal annealing at temperatures from 200 °C to 700 °C for 30 minutes compared with the as-deposited sample. A low magnification image of the sample annealed at 700 °C is included and is the un-labelled image in the above set of images.

7.2 IMPLANTATION RESULTS

Due to the negative results of layer in-diffusion of silver into silicon carbide as discussed above, further studies were performed to try and elucidate the diffusion mechanism. In these experiments, silver was implanted into SiC. For this purpose 360 keV $^{109}Ag^{+}$ with a fluence of 2×10^{16} cm^{-2} was implanted in single crystal 6H SiC wafers at room temperature (23 ^{o}C), at 350 ^{o}C and at 600 ^{o}C. To reduce channelling during implantation, a tilt angle of 7^{o} relative to the normal was used. To avoid excessive beam induced target heating, the flux was kept below 10^{-13} $cm^{-2}s^{-1}$.

To investigate the diffusion behaviour of silver and annealing of radiation damage, the implanted samples were vacuum annealed in a computer controlled *Webb 77 Vacuum Furnace* for different annealing time cycles, i.e. 10 h cycles and 30 minute (min) cycles from temperatures below the melting point of silver (960 ^{o}C) up to 1600 ^{o}C.

The diffusion behaviour, production, and annealing of radiation damage results are discussed as follows: 7.2.1 considers the room temperature implantation results while 7.2.2 discusses the high temperature (350 ^{o}C and 600 ^{o}C) implantation results.

7.2.1 ROOM TEMPERATURE IMPLANTATION

In this section the results of silver implanted into 6H-SiC at room temperature are discussed. They are organised into subsection 7.2.1.1, which considers the radiation damage and the annealing of radiation damage; and subsection 7.2.1.2 which discusses the results of the diffusion experiments.

7.2.1.1 RADIATION DAMAGE RESULTS

The channelled spectrum of the as-implanted silver at room temperature is illustrated in figure 7-2. Also depicted are the random spectrum and the spectrum of an unimplanted sample, with the channelled spectrum and unimplanted spectrum normalised to the random spectrum for comparison. The backscattered yield/counts in the as-implanted channelled spectrum of the implanted sample correspond to damage created during implantation. The region where the channelled spectrum overlaps with

the random spectrum is an amorphous one caused by implantation damage. The depth of this region is approximately 270 nm. Comparing this depth with the typical R_p=*109 nm* and ΔR_p = *39 nm* of silver profile, it becomes clear that implanted silver is embedded within the amorphous region. The amorphous width (or depth) of the amorphous layer is measured as the width between the half maximum of Si surface signal and the half maximum of the Si signal when it decreases at the end of the amorphous layer as illustrated in figure 7-2. Therefore, 6H-SiC implanted at room temperature consists of an amorphous region indicated by *width* - in Figure 7-2, the crystalline or bulk region indicated by *cr* and the interface labelled by *B* (the region between the amorphous layer and the bulk region).

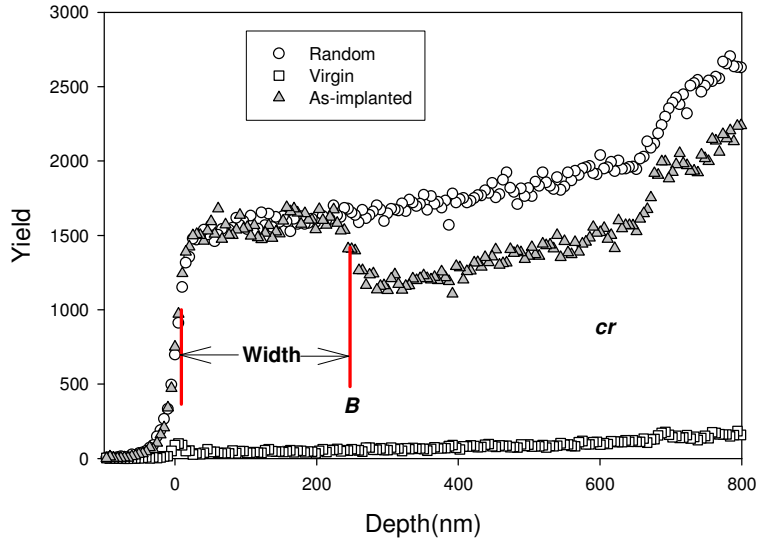

Figure 7-2: Random and aligned backscattering spectra of SiC from 6H-SiC implanted at room temperature with a fluence of 2×10^{16} cm^{-2} compared with the aligned/channelled spectrum of the virgin sample. The α–particle energy was 1.6 MeV and the scattering angle was 165°.

In the initial experiments, 6H-SiC samples implanted at room temperature were sequentially annealed at 960 °C for 2h, 1500 °C for 10 h and 1600 °C for 10 h. The results are shown in figure 7-3. Annealing at 960 °C for 2 h causes an epitaxial re-growth from the bulk to reduce the width of the amorphous region from 270 nm to about 265 nm while at 1500 °C for 10h it further reduces to approximately 220 nm. At 1600 °C for 10 h, the crystallinity of the amorphous region is nearly recovered with

some defects still remaining. The higher de-channelling in the spectrum of the sample annealed at 960 °C might be due to the variations in the crystal alignment.

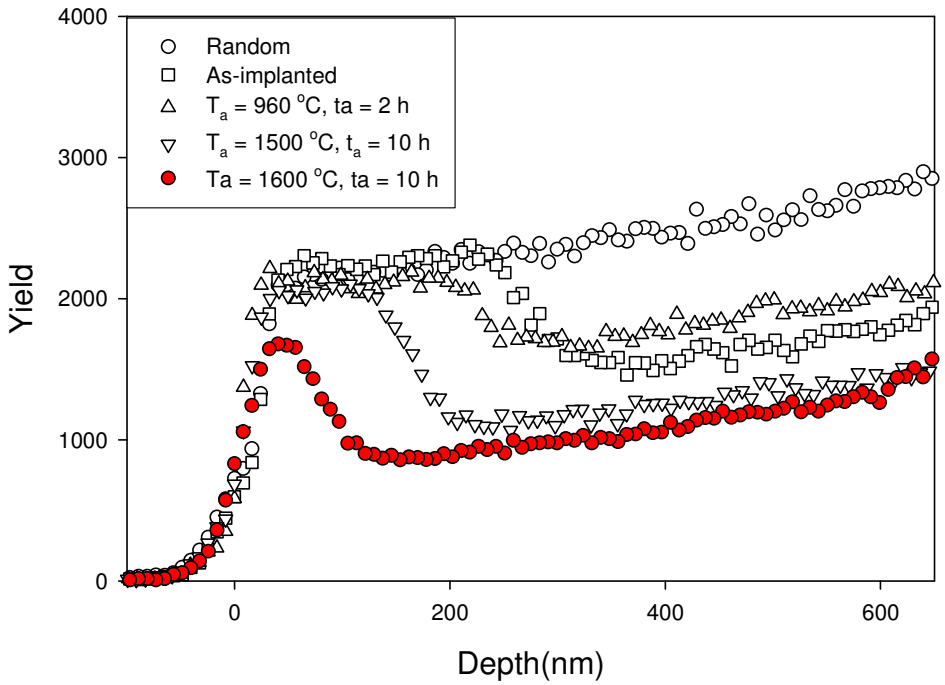

Figure 7-3: Random and aligned backscattering spectra of SiC from 6H-SiC implanted at room temperature (23 °C) and submitted to sequential annealing at 960 °C for 2 h, at 1500 °C for 10 h and at 1600 °C for 10 h.

For the isochronal study, new samples implanted at room temperature were annealed for 10 h at temperatures of 1100 °C, 1200 °C, 1300 °C and 1400°C. The results are to be seen in figure 7-4. Annealing of samples at 1100 °C and 1200 °C causes an epitaxial re-growth from the bulk to reduce the width of the amorphous region from 270 nm to about 240 nm, while annealing at 1300 °C and 1400 °C reduced the amorphous width to 180 nm and 92 nm respectively. These results imply that at 1100 °C and 1200 °C re-crystallization occurs at the same rate. The rate increases with temperatures above 1200 °C, displaying a further reduction of amorphous width at 1300 °C and 1400 °C.

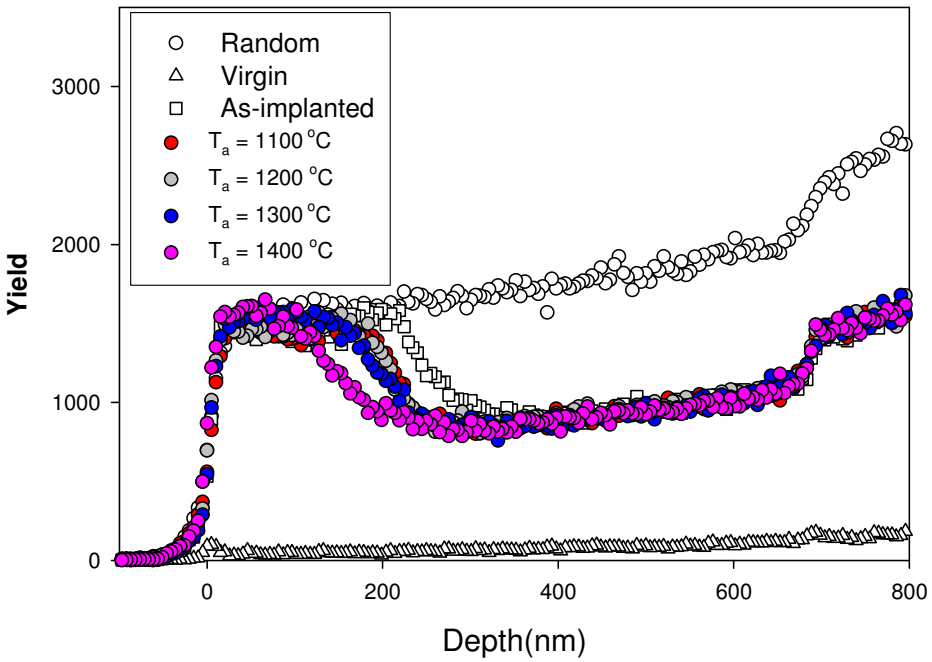

Figure 7-4: *Random and aligned backscattering spectra of SiC for new 6H-SiC implanted at room temperature (23 °C) and submitted to isochronal annealing at 1100 °C, 1200 °C, 1300 °C and 1400 °C for a 10 hours cycle compared with the virgin 6H-SiC aligned spectrum.*

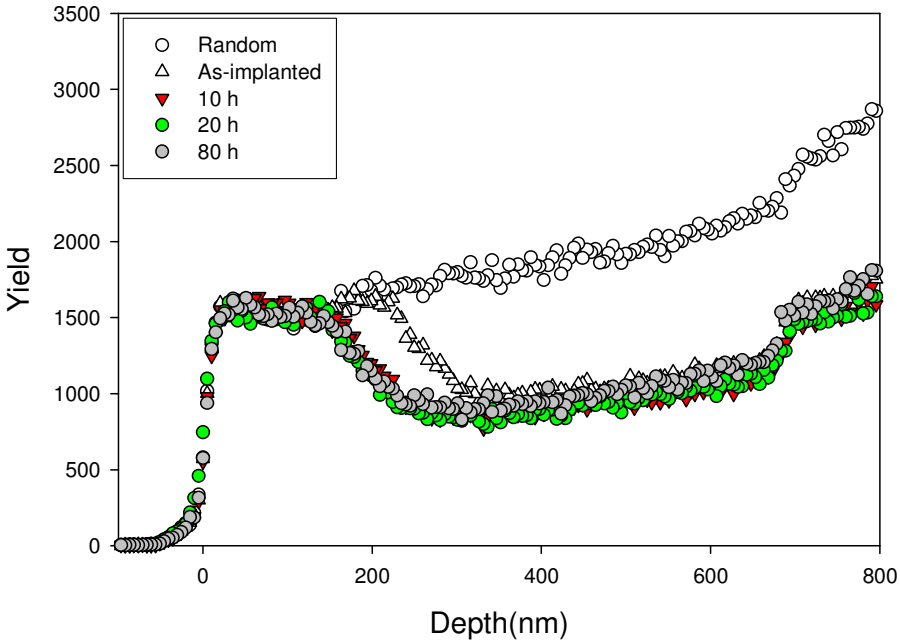

Figure 7-5: Random and aligned backscattering spectra of SiC from 6H-SiC implanted at room temperature (23 °C) and submitted to isothermal annealing at 1300 °C for 10 hours cycles up to 80 h; the 40 h aligned spectrum is not shown.

Isothermal annealing of the sample implanted at room temperature at 1300 ^{o}C for 10 h cycles up to 80 h demonstrates that the amorphous region is reduced from 270 to 180 nm during the first annealing cycle and does not decrease with further annealing at the same temperature (see figure 7-5). Isothermal annealing of the sample implanted at room temperature at 1350 ^{o}C for 30 minutes reduced the amorphous layer to about 220 nm. This depth remained constant with further annealing at 1350 ^{o}C (see figure 7-6). These results indicate that more re-crystallization occurs during a longer annealing time (10 h) compared to the shorter annealing period (30 min) since the difference in temperature between these cases is small.

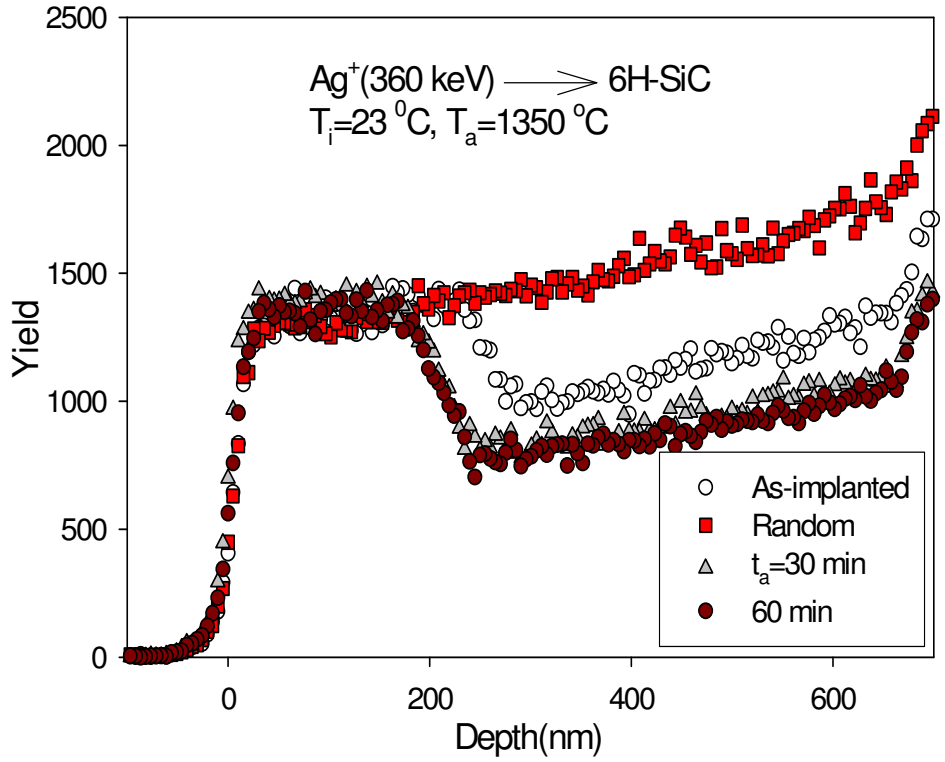

Figure 7-6: Random and aligned backscattering spectra of SiC from 6H-SiC implanted at room temperature (23 ^{o}C) and submitted for isothermal annealing at 1350 ^{o}C for a 30 minutes cycle.

Further investigation of the sample annealed at 1300 ^{o}C for 80 h was performed using Raman scattering spectroscopy to ascertain whether or not the sample was still amorphous (after the first annealing cycle) as suggested by the RBS channelling. This was performed by comparing its results with those of the other samples listed below.

Raman scattering at a visible wavelength (514.5 nm) was performed on the following 6H-SiC samples:

- unimplanted;
- implanted with silver at room temperature; and
- the sample implanted with silver which was annealed at 1300 ^{o}C for 80 h.

The Raman spectra are depicted in figure 7-7. The spectrum for unimplanted 6H-SiC exhibited the characteristic Raman modes for perfect 6H-SiC [Fen99]. After silver implantation at room temperature, three broad Raman bands appeared, with the bands centred around 500, 800 and 1420 cm^{-1}. These broad peaks are caused by Si-Si, Si-C and C-C vibrations, respectively [Fen99]. These bands indicate a loss of 6H-SiC crystallinity and the formation of an amorphous phase as a result of ion implantation. During the amorphization, bonds are formed between Si-Si and C-C, in contrast with crystalline SiC where only Si-C bonds occur. After annealing at 1300 ^{o}C for 80 h the broad peaks disappeared while the Raman spectrum for 6H-SiC reappears. This indicates the recovery of the SiC crystalline structure due to annealing at 1300 ^{o}C for 80 h. A comparison of the Raman intensity of the virgin sample with the Raman intensity of the sample annealed at 1300 ^{o}C for 80 h in figure 7-7 shows that defects are still present in the annealed sample (the lower relative Raman intensity means defects in SiC).

From the Raman results of samples implanted at room temperature and annealed at 1300 ^{o}C for 80 h, it is evident that the sample is no longer amorphous but that defects are still present. However, these results contradict the channelling results of the sample-see figure 7-5. This contradiction could be due to the fact that during the first annealing cycle the amorphous layer was annealed into smaller crystals or crystallites that are randomly orientated or misoriented to the substrate, which resulted in the seemingly amorphous layer in channelling results. The same channelling results could be achieved if, during the first cycles, the amorphous layers re-crystallized to other polytypes of SiC such as 3C-SiC, as suggested by Nakamura et al. [Nak02]. Nakamura et al. found that the annealing of amorphised 6H-SiC leads to the re-growth of the micro-twinned 3C-SiC crystals.

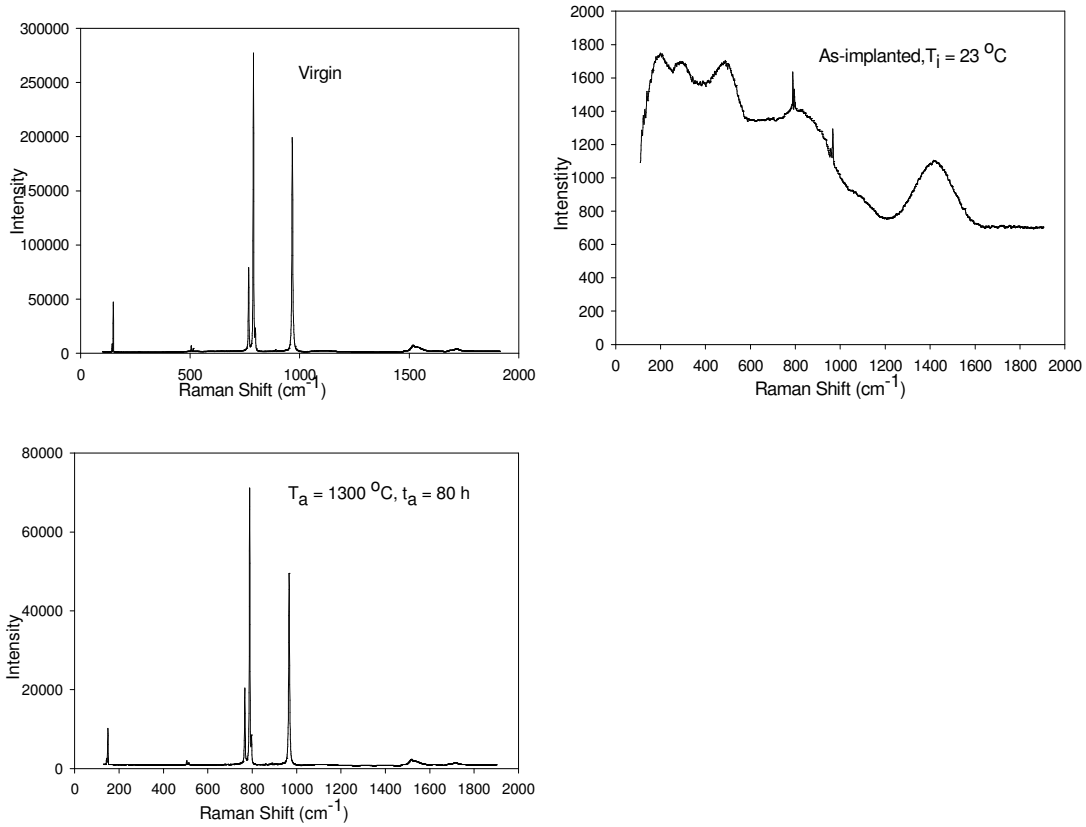

Figure 7-7: Comparative Raman spectra from un-implanted (virgin) 6H-SiC, silver implanted into 6H-SiC at room temperature (23 °C) and after annealing at 1300 °C for 80 h.

Sequential isochronal annealing (for 30 minute cycles) of samples implanted at room temperature at the temperatures 700 °C, 800 °C, 900 °C, 1000 °C, 1100 °C, 1200 °C, 1300 °C, 1400 °C, 1500 °C and 1600 °C indicates that epitaxial re-growth is already taking place at 700 °C (see figure 7-8(a) and figure 7-8(b)). The widths of the amorphous layer (measured as shown in figure 7-2) were plotted as functions of the annealing temperatures in figure 7-8(b). Annealing of the sample at 700 °C decreases the width of the amorphous layer from 270 to about 250 nm. This amorphous width remains at about 250 nm up to 1400 °C where it further decreases to about 204 nm. At 1500 °C it decreases to about 170 nm. The crystal structure appears to be recovered after annealing at 1600 °C but with more carbon being detected at this temperature. This might be due to decomposition of SiC at this temperature, which allows Si to evaporate since this temperature is well above the melting point (1411 °C) of Si. No signal from the implanted Ag was observed in the RBS spectrum. This could indicate that the top amorphous layer is thermally etched away or sublimated during annealing, as was suggested by Wendler et al. and Rao [Wen98][Rao03]. Therefore, the decrease

in the width of the amorphous layer at low temperatures might be due either to an epitaxial re-growth from the amorphous/bulk interface as can be seen in figure 7-8(a) or to the sublimation of the (top) amorphous layer during annealing. At the temperatures where epitaxial re-growth did not occur as observed by channelling, this result might imply that the amorphous layer re-crystallised to other polytypes as explained above, while the thermal etching was negligible at those temperatures.

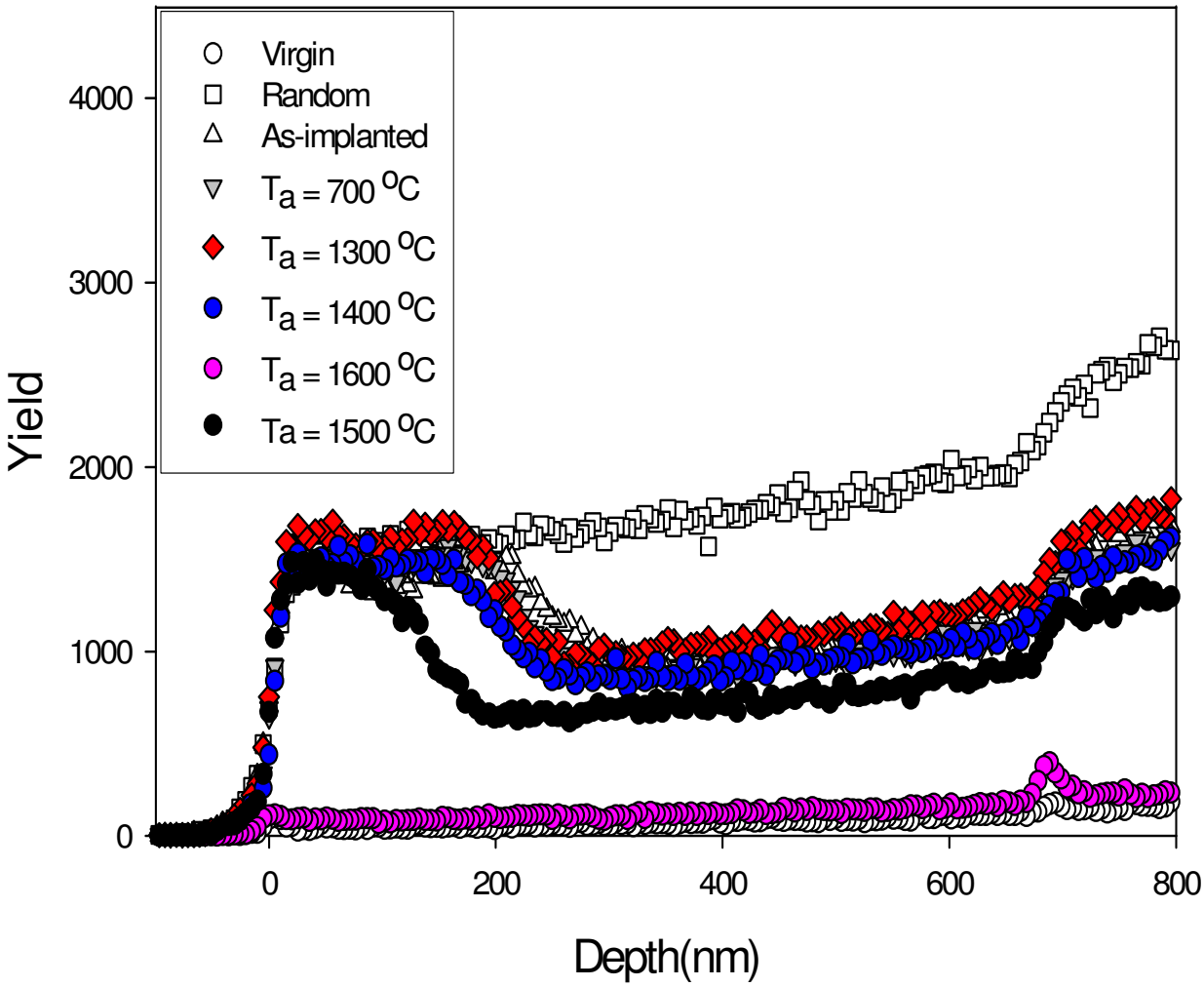

Figure 7-8(a): Random and aligned backscattering spectra of SiC from 6H-SiC implanted at room temperature (23 °C) and isochronally annealed at temperatures from 700 °C to 1600 °C for 30 minutes cycles.

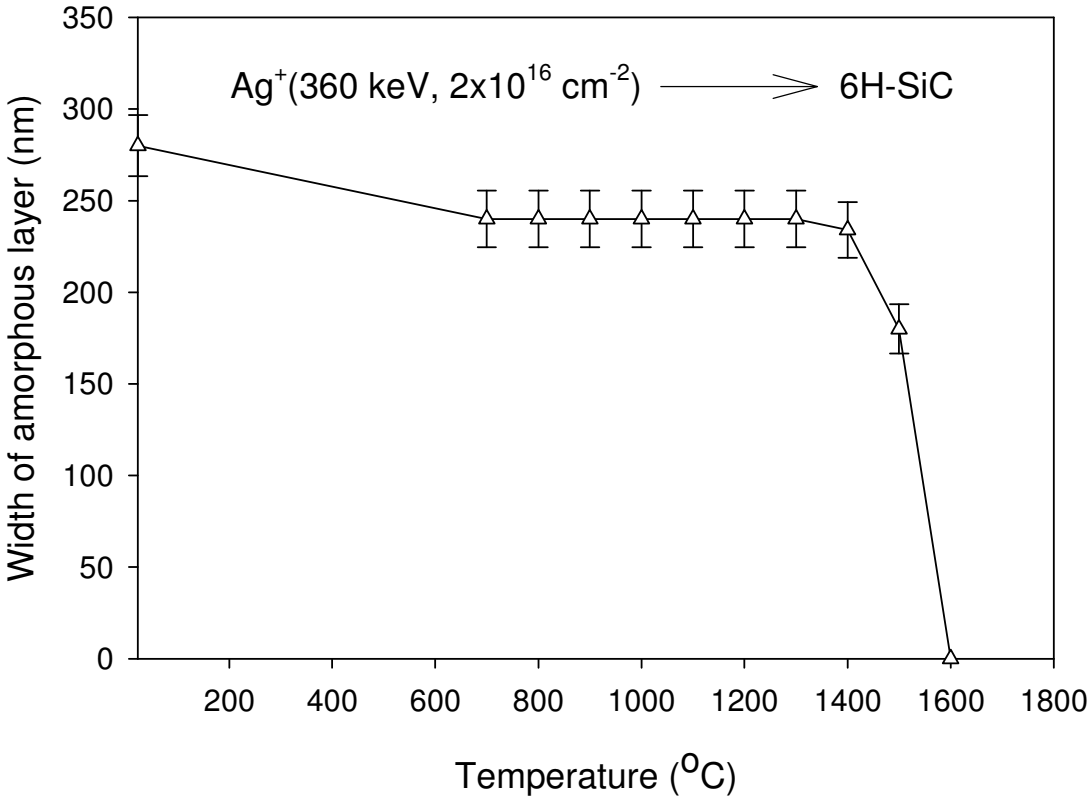

Figure 7-8(b): The width of the amorphous layer as a function of annealing temperatures during the isochronal sequential annealing from 700 °C to 1600 °C for 30 minute cycles.

In summary, our production of radiation damage during the implantation results of this study is in agreement with the results of Wendler et al. [Wen98]. Wendler et al. have shown that for high energy ion damage, amorphization is not achieved for implantation temperatures above 250 °C. Furthermore, the annealing of radiation damage produced during implantation results is in agreement with Bohn et al. [Boh87] and Pacaud et al. [Pac96]. Bohn et al. found that the amorphous layers re-grew epitaxially from the underlying undamaged material up to 1500 °C, above which the damage annealed rapidly in a narrow temperature interval while Pacaud et al. showed that annealing of the amorphous layer cannot be achieved at the temperature of 1500 °C. Decomposition of SiC, resulting in the excess of carbon on the SiC, is found to be taking place at 1600 °C. This is caused by silicon evaporating at 1600 °C, leaving excess carbon and thus causing lager carbon peak on the SiC RBS spectrum.

7.2.1.2 IMPLANTED LAYER DIFFUSION RESULTS

Measurements to determine silver diffusion in 6H-SiC were performed simultaneously with the annealing of radiation damage discussed above, using random spectra from the RBS. A typical profile of silver implanted at room temperature as compared with TRIM 98 prediction is depicted in figure 7-9, where the fluence (ϕ), experimental and TRIM 98 moments are also shown. By comparing the experimental moments with TRIM 98 ones, it became quite clear that the measured projected range of silver peak is about 2% deeper, which is within TRIM calculation error of 5 %. The typical FWHM of silver peak is about 63 % wider as compared to the TRIM 98 results but the concentration is the same in both peaks. This difference in FWHM causes the silver concentration of the TRIM simulation to be higher than the measured one around the projected range (see figure 7-9). This discrepancy is caused by the fact that TRIM does not take into account the crystal structure or dynamic composition changes in the material that occur when the ion penetrates materials; however, approximations are used in this program. These include the following:

- binary collision (i.e. the influence of neighbouring atoms is neglected);
- recombination of knocked off atoms (interstitials) with the vacancies is neglected;
- the electronic stopping power is an averaging fit to a large number of experiments;
- the interatomic potential as a universal form which is an averaging fit to quantum mechanical calculations;
- the target atom which reaches the surface is able to leave the surface (be sputtered) if it has sufficient momentum and energy to pass the surface barrier.

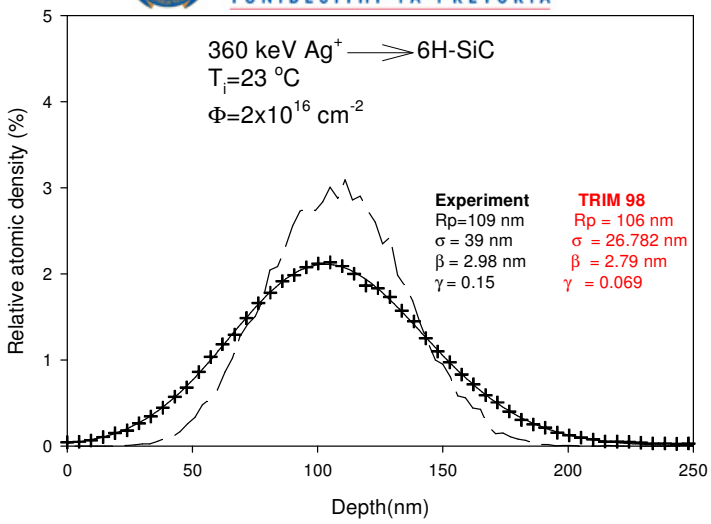

Figure7-9: Silver depth profile in 6H-SiC implanted at room temperature as determined by RBS. The broken line is the theoretical distribution obtained with the TRIM-98 code.

The silver depth profiles in 6H-SiC implanted at room temperature after sequentially annealed at 960 °C for 2 hours, 1500 °C for 10 hours and 1600 °C for 10 hours as compared with the as-implanted profile are illustrated in figure 7-10. Annealing at 960 °C narrows the silver profile's width, causing the concentration to be greater at the centre compared to that of the as-implanted profile (see figure 7-10). Similar results could be achieved if the silver were to form a precipitate at this temperature. If the same sample (that was annealed at 960 °C) is further sequentially annealed at 1500 °C and 1600 °C for 10 hours, the silver profile tends to shift without any broadening toward the surface at 1500 °C with 2 % of silver loss from the surface (the amount of silver detectable by RBS is proportional to the area under the silver curve.). At 1600 °C more than 50% of the silver is lost from the surface. From the shape of the distribution and from fitting the profile to an Edgeworth function, as discussed in section 5.6, it is clear that no detectable Fickian-type diffusion into the bulk or towards the surface is taking place. The shift of silver profile towards the surface and subsequent loss at higher temperatures might be due to material (SiC) being removed from the surface during annealing at these temperatures. This will be discussed as this section progresses. These diffusion results seem to be supporting the suggestion that the ion bombardment-induced amorphous SiC layer is no longer amorphous (after annealing at 1300 °C for 80 h) as discussed in section 7.2.1.1, but re-crystallized to other polytypes of SiC such as 3C-SiC through which silver does not diffuse.

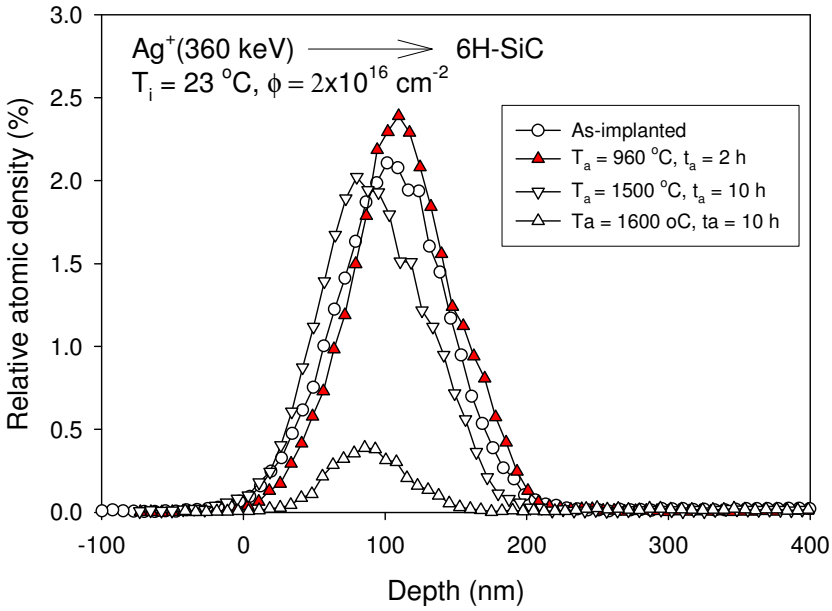

Figure 7-10: Silver depth profiles of 6H-SiC implanted at room temperature after annealing at 960 °C for 2 hours, 1500 °C for 10 hours and 1600 °C for 10 hours.

Owing to the unexpected results of our initial diffusion experiments, silver diffusion in single crystal 6H-silicon carbide was investigated further by isochronal annealing of new samples at 1100 °C, 1200 °C, 1300 °C and 1400 °C for 10 hours, so that the results of annealing at higher annealing temperatures are not influenced by lower annealing temperatures as in our previous experiments. Therefore, in these experiments all samples were initially amorphised SiC while in the former experiments the samples were only amorphous during annealing at a lower temperature, i.e. 960 °C. The results of the isochronal annealing experiments are illustrated in figures 7-11 to 7-13. Silver loss starts at 1100 °C (see figure 7-12), while silver diffusion in amorphous SiC accompanied by silver loss from the surface begins at 1300 °C (figure 7-11). The silver profile maintains a symmetrical shape with less than 30% of silver lost from the surface. The silver retained ratio was calculated from the total counts/yield of silver after annealing, divided by the counts of the as-implanted silver peaks. At 1400 °C silver diffuses significantly, with the silver profile shifting towards the surface and becoming asymmetric (see figure 7-11). 50% of silver is lost from the surface at 1400 °C. At temperatures below 1300 °C the widths of the silver profiles become narrower and their counts decrease. This is the result of some of the implanted silver forming precipitates, and some silver being lost at these temperatures. The silver precipitates can be seen in the cross sectional SEM image for

a sample implanted at room temperature and then annealed at 1250 °C for 30 minutes (figure 7-14). This sample in figure 7-14 was prepared by standard TEM sample preparation, i.e. glued on a poly crystalline SiC, together with chemical polishing and ion milling. In figure 7-14, the surface from which implantation was performed is indicated as S, while Ag represents the silver precipitates and Poly SiC represents polycrystalline SiC. This is the proof that below 1300 °C silver forms precipitates, as has been suggested above in this section.

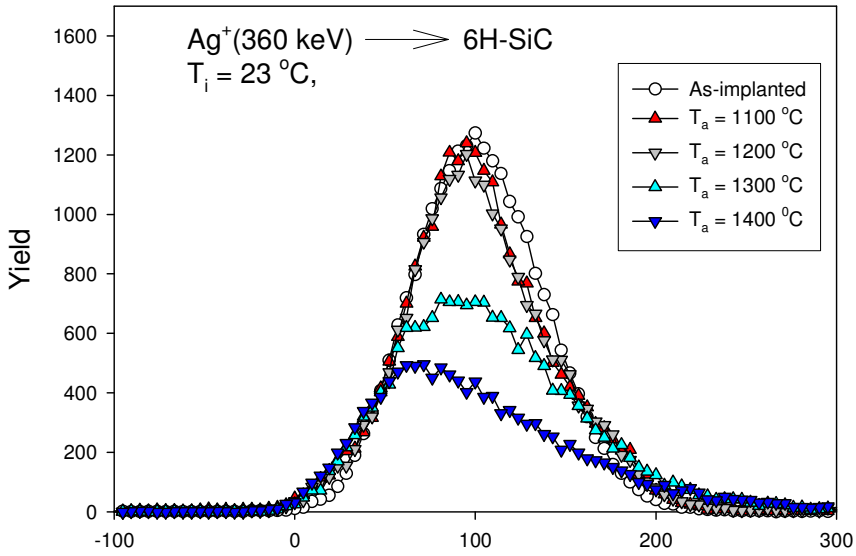

Figure 7-11: Silver depth profiles of 6H-SiC implanted at room temperature after isochronal annealing at 1100 °C, 1200 °C, 1300 °C and 1400 °C for a 10 hours cycle.

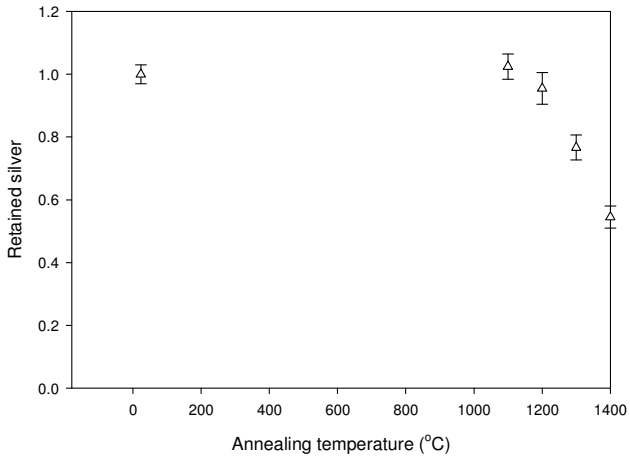

Figure 7-12: Fraction of retained silver in 6H- SiC implanted at room temperature after isochronal annealing at 1100 °C, 1200 °C, 1300 °C and 1400 °C for 10 hours.

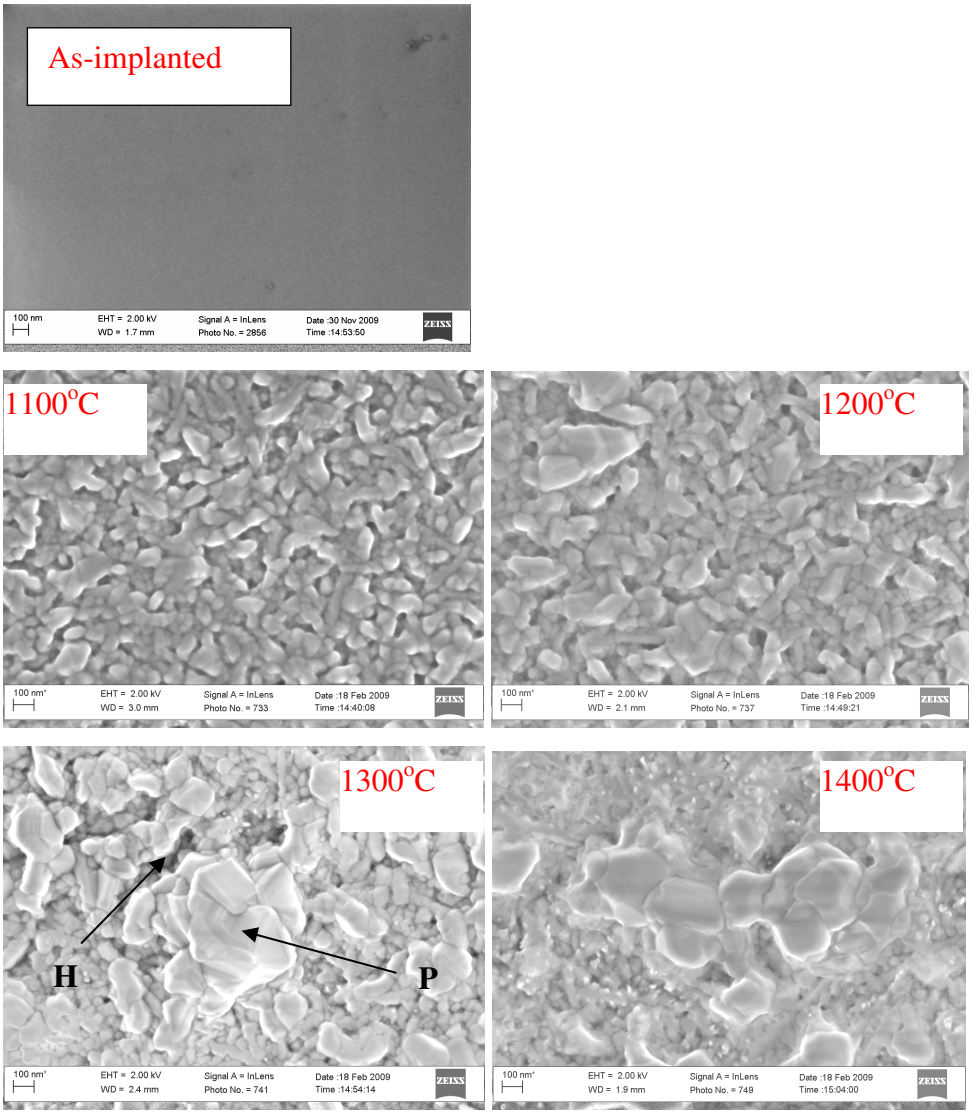

Figure 7-13: SEM images of 6H- SiC implanted at room temperature after isochronal annealing at 1100 °C, 1200 °C, 1300 °C and 1400 °C for 10 hours as compared with as-implanted; the magnification bar is 100 nm in all the images.

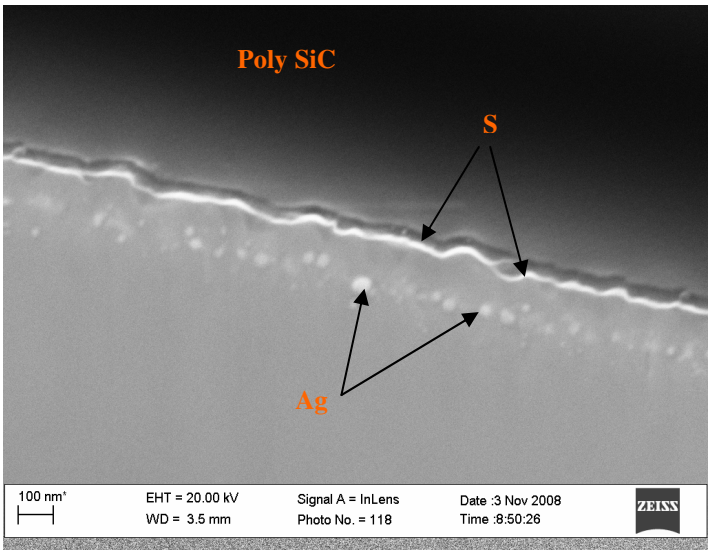

Figure 7-14: The cross sectional image of 6H-SiC implanted with silver at room temperature after annealed at 1250 °C for 30 minutes. This sample is glued to poly-SiC.

The asymmetry of the silver profile at 1400 ^{o}C is due to silver loss from the surface accompanied by diffusion and some changes on the silicon carbide surfaces occurring during annealing as seen in figure 7-13. Figure 7-13 depicts SEM images of samples after isochronal annealing at 1100 ^{o}C, 1200 ^{o}C, 1300 ^{o}C and 1400 ^{o}C for a 10 hours cycle as compared to an as-implanted sample.

The surface of the SiC implanted at room temperature was fairly smooth and amorphous compared to the SiC after annealing as perceived from Figure 7-2 and 7-13. Annealing of the amorphised SiC at 1100 ^{o}C causes the formation of silicon carbide crystals on the surface. These crystals increase in size together with increasing annealing temperature up to 1300 ^{o}C. Some large protrusions (P) also appear at this temperature. Holes (H) are also visible on the silicon carbide surface after annealing. These holes become larger at 1300 ^{o}C where the loss of silver is noticeable. Thus, the silver escapes through these holes, thereby explaining the loss of the implanted silver through the surface without showing the expected diffusion broadening of the implanted profile. (Note that the projected range of the implanted silver is approximately 100 nm – the size of the scale bar in the SEM images.) At 1400 ^{o}C, the larger protrusions are thermally etched and the implanted silver becomes closer to the surface (figure 7-11). This thermal etching could explain the shift of silver towards the surface at 1400 ^{o}C (figure 7-11) and at 1500 ^{o}C (figure 7-10). The discrepancy in broadening of silver peak and silver lost between the two results, i.e. those in figure 7-10 and figure 7-11, is caused by the conditions of the annealing experiments as explained earlier in this section. For the figure 7-10 results the sample was no longer amorphous during annealing at higher temperatures while in the results of figure 7-11 the samples were amorphous during annealing at all the temperatures.

To further investigate the diffusion of silver in 6H-SiC implanted at room temperature, a temperature of 1300 ^{o}C was chosen for the isothermal annealing investigation because the rate of profile broadening was reasonably large and silver loss (less than 30%) from the surface was still acceptable. Silver profiles and their measured widths after annealing between 10 to 80 hours are depicted in figures 7-15 and 7-16. An increase of the width of the silver profile occurred after the first annealing cycle of 10 hours. Further annealing did not alter the width of the silver profile any further. This indicates that the diffusion of silver only took place during

the initial stages of annealing. This could be due to radiation damage-induced diffusion, since implantation at room temperature resulted in the silver being initially embedded in amorphous SiC. The fact that the measured widths remain constant for annealing times longer than 10 hours at 1300 ^{o}C suggests that the amorphous state which allows diffusion of silver is no longer available. This seems to contradict the channelling results which indicate that the damage density was the same as that in the initial amorphous layer (see figure 7-5). However, if the amorphous SiC layer is annealed during this first annealing cycle to form small crystals or crystallites that are randomly orientated or misorientated to the substrate, the channelling spectrum will be similar to that of an amorphous layer. The silver diffusion mechanism will nevertheless alter dramatically between these two substrates, thereby explaining the above results. This explanation is fully supported by the Raman results (see figure 7-6) and is in line with the asymmetric shape of the room temperature implanted silver profile after annealing at 1400 ^{o}C, compared to the symmetric profiles obtained after annealing for 10 h at much higher temperatures, viz. 1500 and 1600 ^{o}C: see Figure 7-10. The asymmetric RBS profile of the sample annealed at 1400 ^{o}C (see Figure 7-11) is caused by silver loss accompanied by diffusion in amorphous SiC since the sample was directly annealed at this temperature while the symmetric profiles at 1500 and 1600 ^{o}C are due to the fact that the sample was sequentially annealed from lower temperatures. This hinders diffusion of silver at these higher temperatures as explained in the section above. At the higher annealing temperatures there is a substantial loss of silver from the SiC substrate through the surface. This will reduce the concentration on the surface side of the silver profile, resulting in a more symmetric profile at these higher temperatures. However, an alternative investigating technique such as TEM is necessary to clarify the nature of the damage after the first annealing step and either prove or disprove this explanation. Based on the RBS and Raman results and the above discussion it can be assumed that this initial diffusion of implanted silver is due to the amorphous SiC layer.

The diffusion coefficient obtained from fitting the experimental data for t > 10 hours to a straight line as a function of time yields an upper limit of: $D < 10^{-21}\ m^2 s^{-1}$ at 1300 ^{o}C, which is in the same range as that obtained by MacLean et al [Mac06], who found a value of $D < 5\times10^{-21}\ m^2 s^{-1}$ at 1500 ^{o}C.

From the initial slopes of FWHM squares as a function of annealing time, effective diffusion coefficients of silver could be calculated but this would require detailed knowledge of the structural evolution of the SiC during the first annealing cycle (10 hours cycle). Due to the lack of knowledge regarding this evolution the annealing cycle was reduced to obtain the diffusion during the first cycle, thereby avoiding annealing of the radiation damage which would cause silver diffusion to stop.

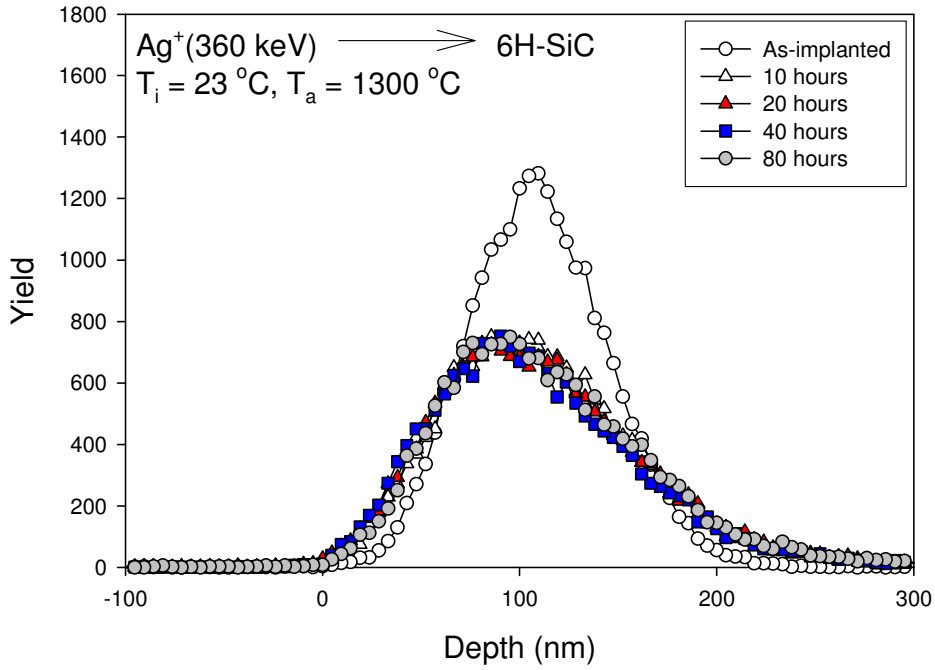

Figure 7-15: Silver depth profiles of 6H-SiC implanted at room temperature after isothermal annealing at 1300 °C for sequential 10 hours cycles up to 80 hours.

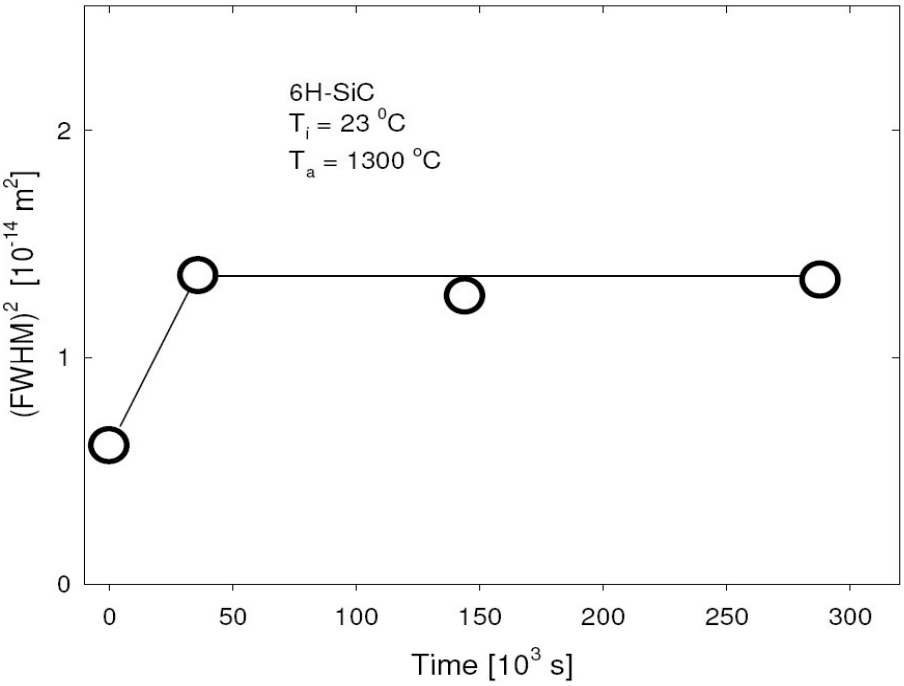

Figure7-16: Square of the full width at half maximum (FWHM) of the silver profile in 6H-SiC as function of isothermal annealing time at Ta=1300 °C for sequential 10 hours cycles up to 80 hours.

The time at which silver diffusion stops or at which most of the annealing of the damage occurred was investigated by performing an isothermal annealing at 1300 °C and 1350 °C for 30 minute cycles up to 120 minutes. The results of the experiments are portrayed in figures 7-17 to 7-19. A relative increase of the FWHM of silver profiles during the first annealing cycles together with a lower increase in width in the second cycles was observed. The sharp increase during the first annealing cycle is without a doubt due to diffusion of the silver in amorphous SiC, while the lower second increase is due to a reduction in the damage, causing less diffusion to occur after the first annealing cycle. For the third cycle the widths at both temperatures remain unchanged, indicating that all the damage which led to the diffusion has been annealed during the first and the second cycles.

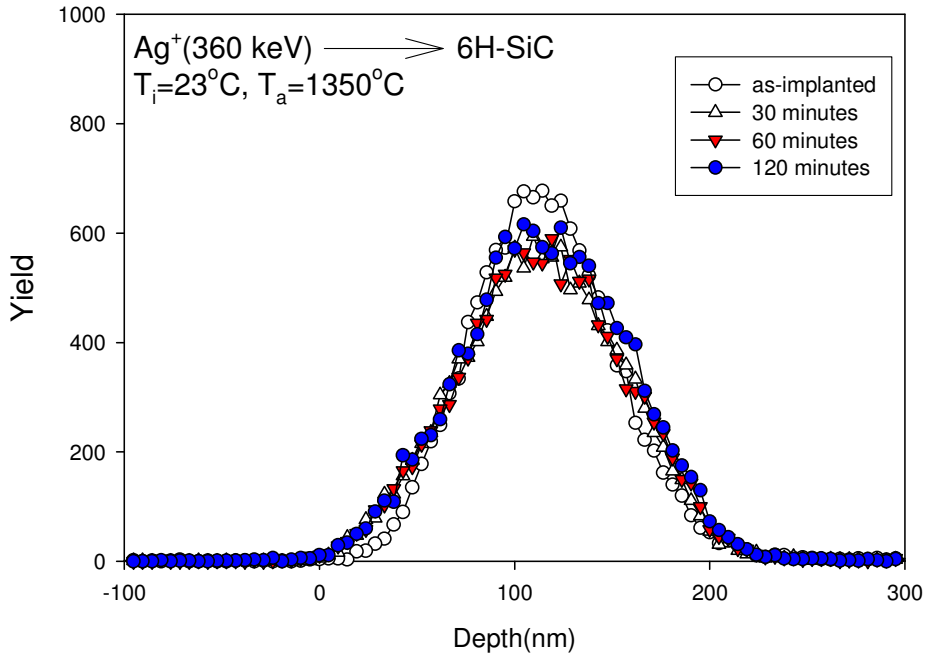

Figure 7-17: Silver depth profiles of 6H-SiC implanted at room temperature after isothermal annealing at 1300 °C for a 30 minutes cycle up to 120 minutes.

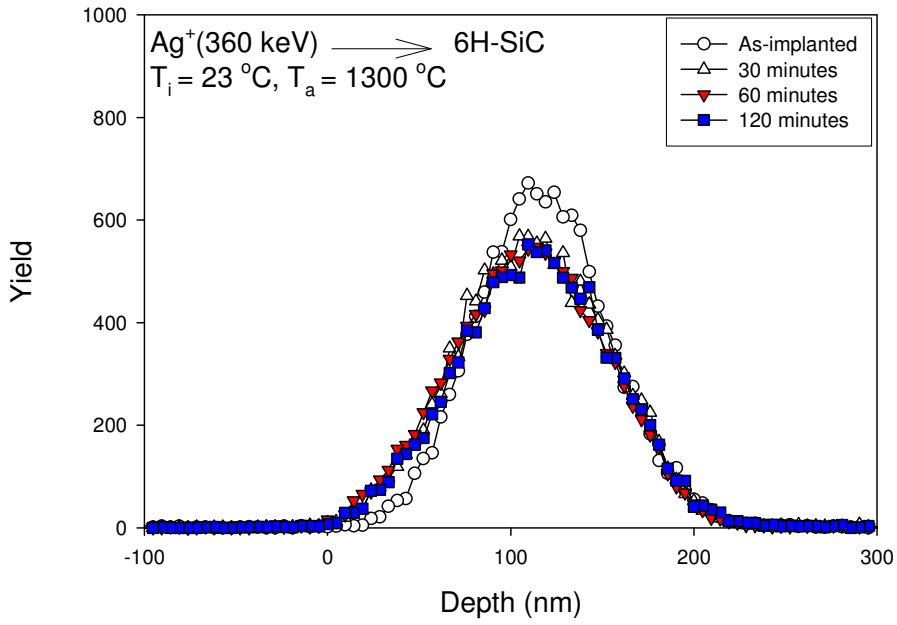

Figure 7-18: Silver depth profiles of 6H-SiC implanted at room temperature after isothermal annealing at 1300 °C for a 30 minutes cycle up to 120 minutes.

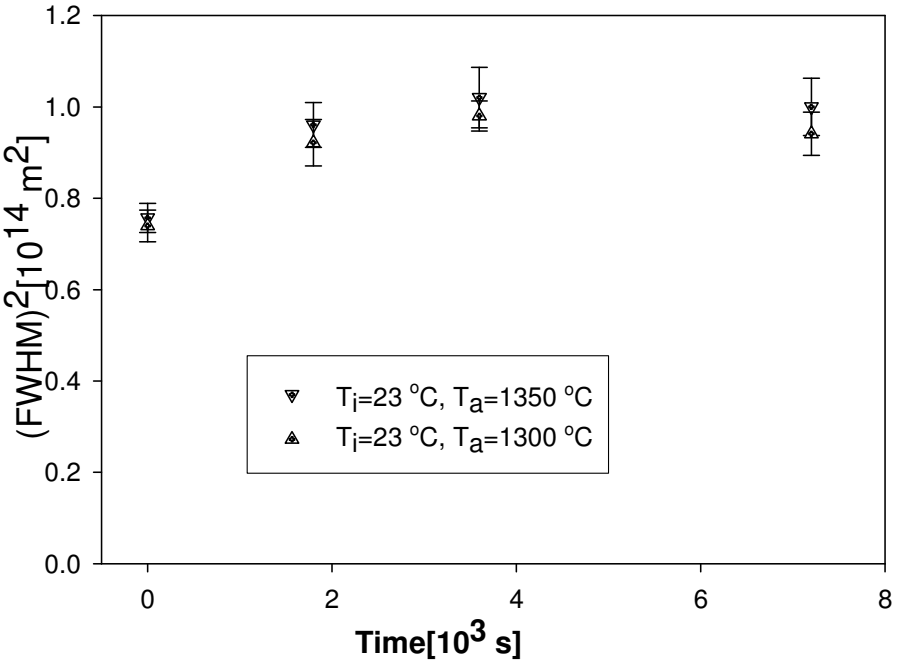

Figure 7-19: Square of the full width at half maximum (FWHM) of the silver profile in 6H-SiC as function of isothermal annealing time (30 minutes) at Ta=1300 °C and 1350 °C.

We have investigated silver diffusion in amorphous SiC for the temperatures where diffusion occurs, viz. between 1300 °C and 1400 °C. This has been carried out by annealing the as-implanted 6H-SiC samples (implanted at room temperature) at 1300 °C, 1315 °C, 1325 °C, 1350 °C, 1365 °C, 1375 °C and 1385 °C for 30 minutes. The silver depth profile results are illustrated in figure 7-20. At these temperatures the profiles are asymmetric due to silver loss accompanied by diffusion. The amount of silver lost during annealing is very small because of the short annealing cycle of 30 minutes. The squares of FWHMs as a function of temperature in the selected range i.e. 1300 °C < 1400 °C are portrayed in figure 7-21. Because of the narrow range of temperature and overshooting of oven temperature during annealing at these temperatures, there are large errors in the measurements.

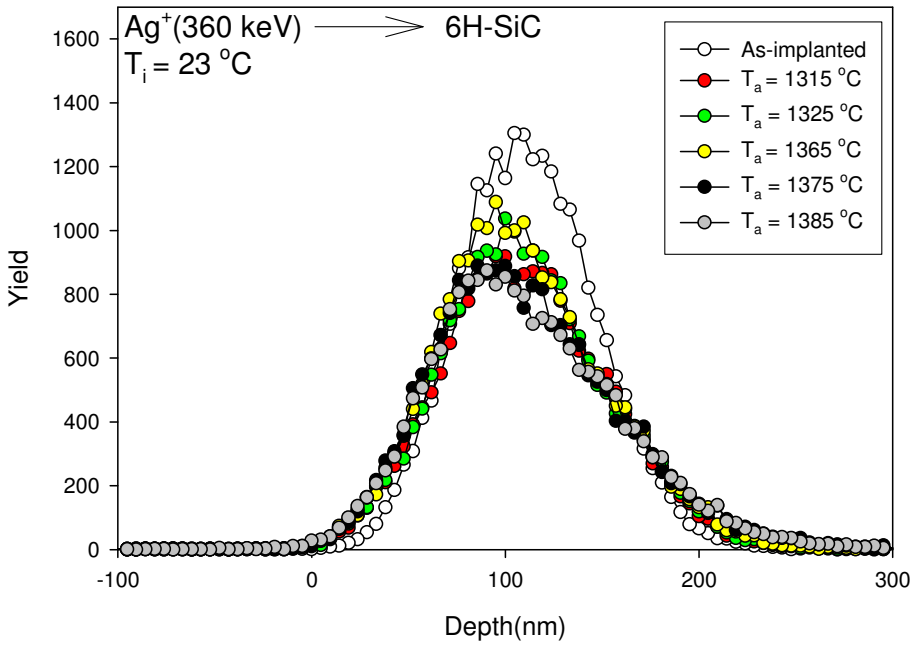

Figure 7-20: Silver depth profiles of 6H-SiC implanted at room temperature after isochronal annealing at 1315 °C, 1325 °C 1365 °C 1375 °C and 1385 °C for a 30 minutes cycle as compared to the as-implanted profile.

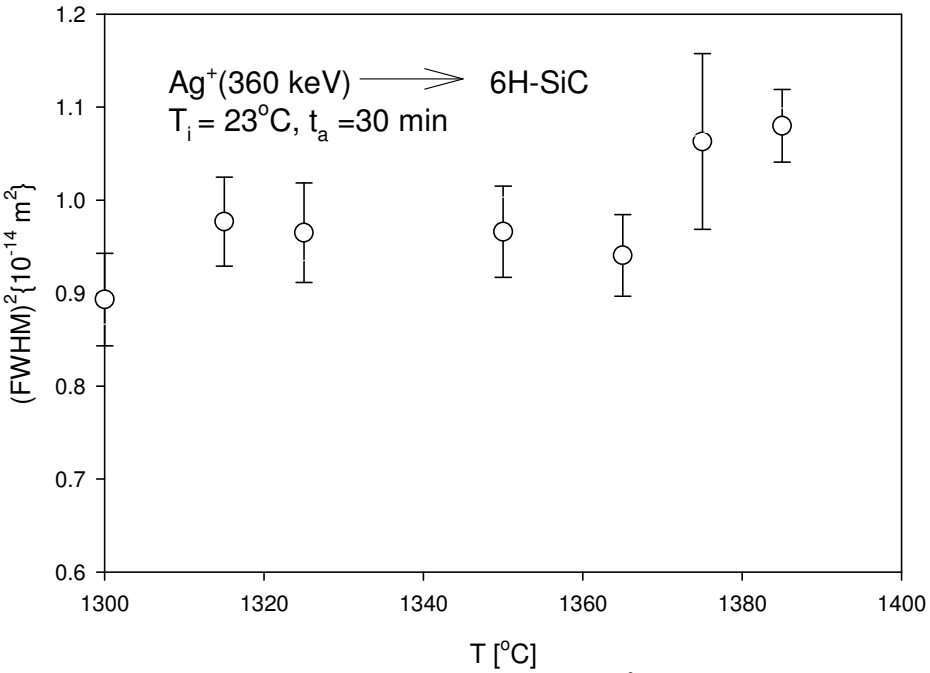

Figure 7-21: Square of the full width at half maximum $(FWHM)^2$ of the silver profile in 6H-SiC as a function of isothermal annealing time (30 minutes) at Ta=1300 °C to 1385 °C.

By comparing the squares of the FWHM of the silver depth profiles after annealing plotted in figure 7-21, with the as-implanted FWHM square, the diffusion coefficients were calculated: they are depicted in figure 7-22. Assuming that the diffusion follows

an Arrhenius type mechanism, the activation energy and pre-exponential factor of silver diffusion in amorphous silicon carbide were determined from an Arrhenius plot. The activation energy E_a and pre-exponential factor (D_o) were calculated from the slope and the y-intercept, respectively. The Arrhenius plot is displayed in figure 7-22. The following values were found: $D_o = 6.6 \times 10^{-12}$ m^2s^{-1} and $E_a = 3.7\times 10^{-19}J$. These are in agreement with the results of silver diffusion in polycrystalline CVD-SiC found by Friedland et al. [Fri09]. These results imply that the diffusion associated with the less dense structure of fully amorphized SiC due to volume swelling is approximately the same as the diffusion of silver via grain boundary diffusion.

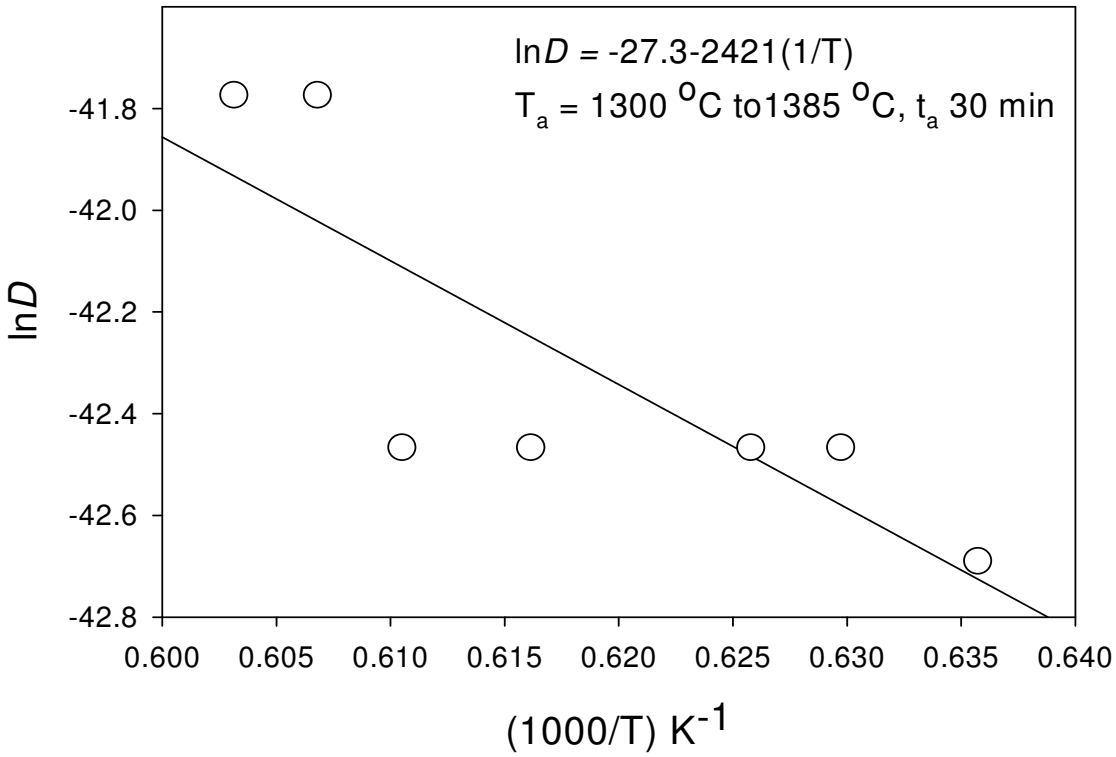

Figure 7-22: Experimental silver diffusion coefficients in amorphous SiC measured in this study from which $D_o = 6.5602 \times 10^{-12}$ m^2s^{-1} and $E_a = 3.69671\times 10^{-19}J$.

Finally, the silver depth profiles collected during the study of annealing of radiation damage by sequential isochronal annealing of the same sample at temperatures between 700 °C and 1600 °C, in 100°C steps, for 30 minutes (subsection 7.2.1.1), also show that diffusion of silver is accompanied by a loss of silver from the surface which

starts at 1300 °C while silver loss begins at lower temperatures (see figures 7-23 to 7-25). The rest of the results are similar to the isochronal results of the 10 hours cycle except that the amount of silver lost at 1300 °C for 30 minutes is less than that at 1300 °C for 10 hours. This is due to the shorter annealing time and the sequential annealing at low temperatures. The silver profiles indicate the decrease in widths at the temperatures below 1300 °C, due to silver forming some precipitates as explained earlier in this section. The silver profile seems to maintain its symmetric shape with the sample annealed at 1400 °C for 30 minutes. This is due to the recrystallization during annealing at the temperatures below 1300 °C for a 30 minutes cycle and the shorter annealing time at 1300 °C since the same sample was sequentially annealed from 700 °C.

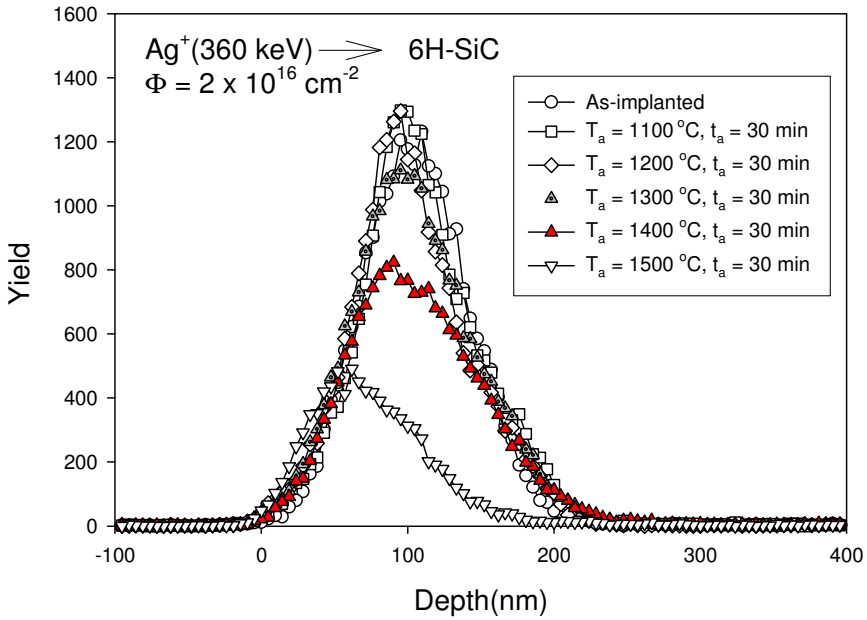

Figure 7-23: Silver depth profiles of 6H-SiC implanted at room temperature after isochronal annealing at 1100 °C, 1200 °C, 1300 °C, 1400 °C and 1500 °C for a 30 minute cycle.

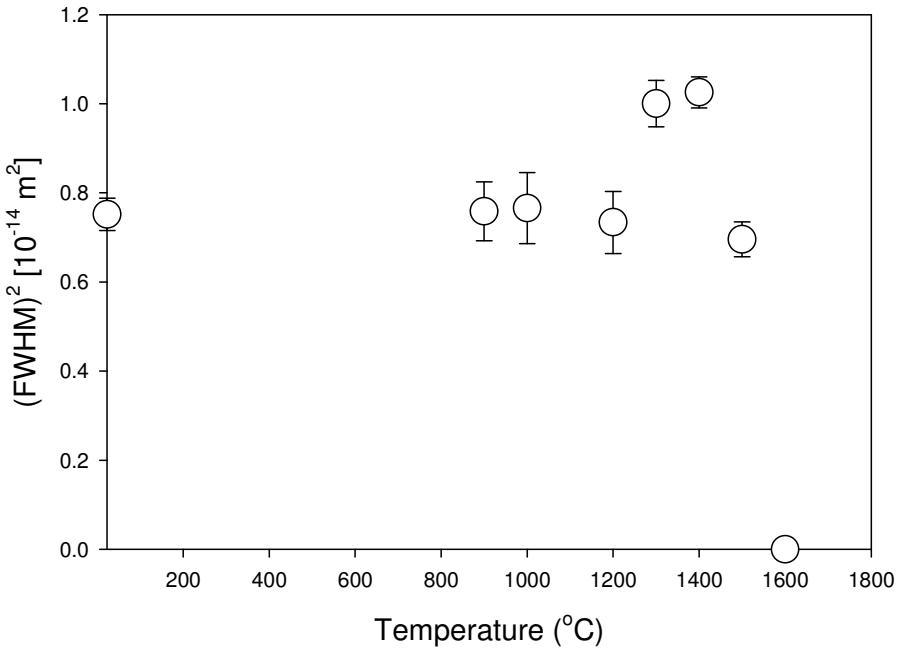

Figure7-24: Square of the full width at half maximum (FWHM) of the silver profile in 6H-SiC as a function of isothermal annealing at temperature 900 °C, 1000 °C, 1200 °C, 1300 °C, 1400 °C, 1500 °C and 1600 °C for 30 minute cycles.

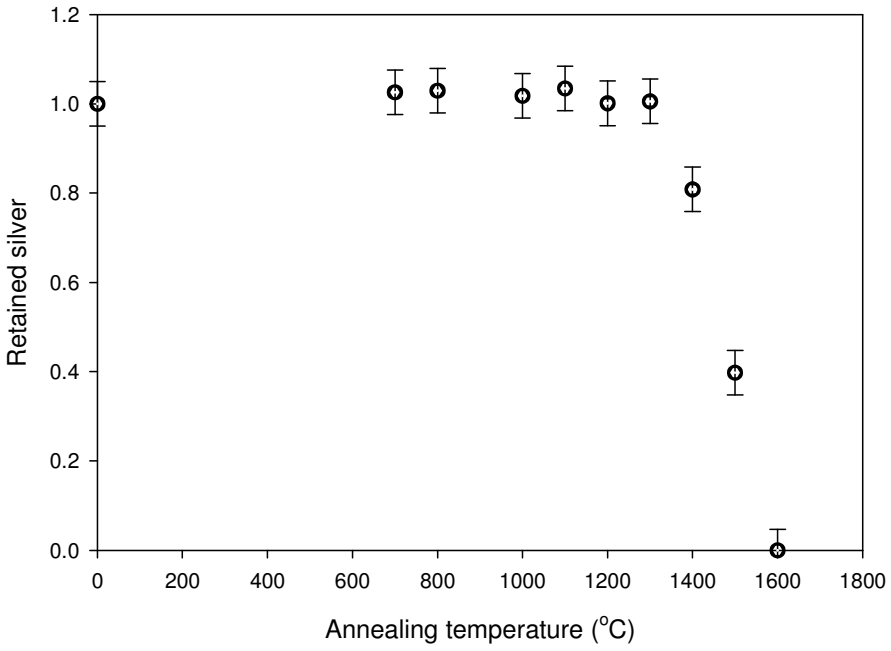

Figure 7-25: Fraction of retained silver in 6H- SiC implanted at room temperature after isochronal annealing at a temperature from 700 °C to 1600 °C for 30 minutes.

7.2.2 HIGH TEMPERATURE IMPLANTATIONS

In this section the results of silver implanted into 6H-SiC at 350 ^{o}C and 600 ^{o}C are discussed. In subsection 7.2.2.1 the radiation damage results are considered while in subsection 7.2.2.2 the diffusion results are discussed.

7.2.2.1 RADIATION DAMAGE RESULTS

Rutherford Backscattering Spectroscopy combined with channelling of alpha particles was used to examine the annealing of radiation damage of silver implanted in 6H-SiC at 350 ^{o}C and 600 ^{o}C. These spectra are compared with the spectrum from an unimplanted sample as shown in figure 7-26. Implantation of silver at 600 ^{o}C retains crystallinity although distortions occur in the implanted region. This is evident from the broad peak around 180 nm in figure 7-26. This damage peak is deeper than the typical projected range R_p= 102 *nm* of the silver peak measured and that predicted by TRIM 98 R_p= 106*nm*. The damage peak predicted by TRIM 98 is at a depth of about 90 nm (see figure 3.10). The discrepancy has already been explained in subsection 7.2.1.2.

Implantation at 350 ^{o}C also retains crystallinity but with more distortions created when compared to silver implanted at 600 ^{o}C. This is caused by the fact that at 600 ^{o}C, the displaced atoms are more mobile because of their higher thermal energy than at 350 ^{o}C. The greater energy increases the probability of the displaced atoms returning to their original lattice sites. These implantation results indicate the irradiation hardness of SiC during implantation at these two temperatures. Similar radiation hardness of SiC above 300 ^{o}C has been reported for other heavy ions [Wen98].

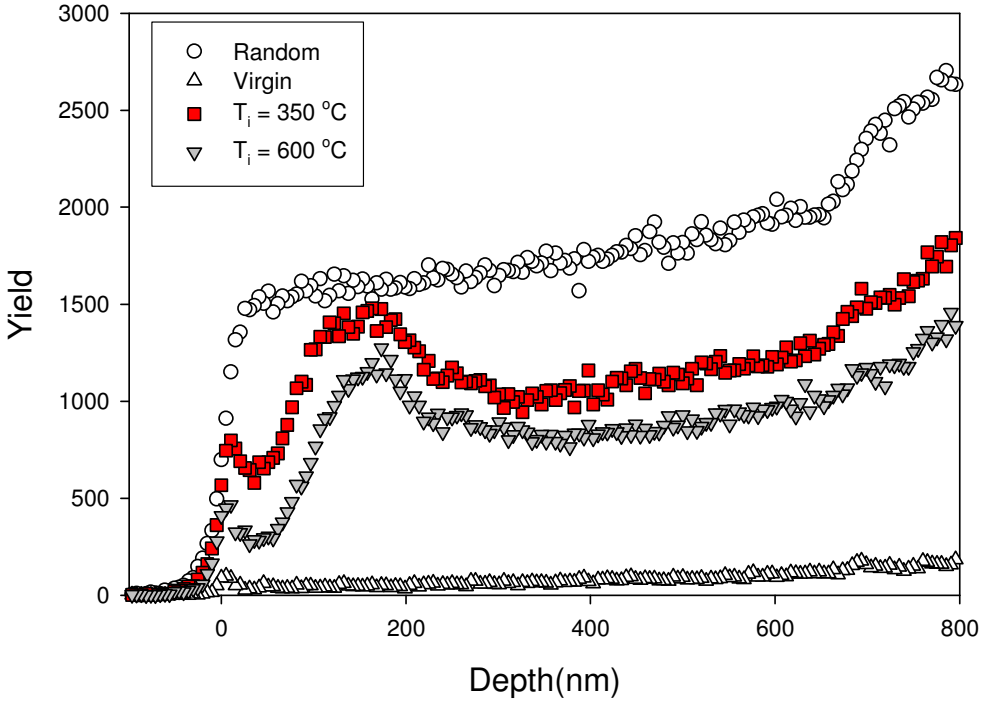

Figure 7-26: Random and aligned backscattering spectra of targets implanted at 350 °C and 600 °C with a fluence of 2×10^{16} $Ag^{+}cm^{-2}$ compared with an unimplanted sample. The α–particles' energy was 1.6 MeV and the scattering angle was 165°.

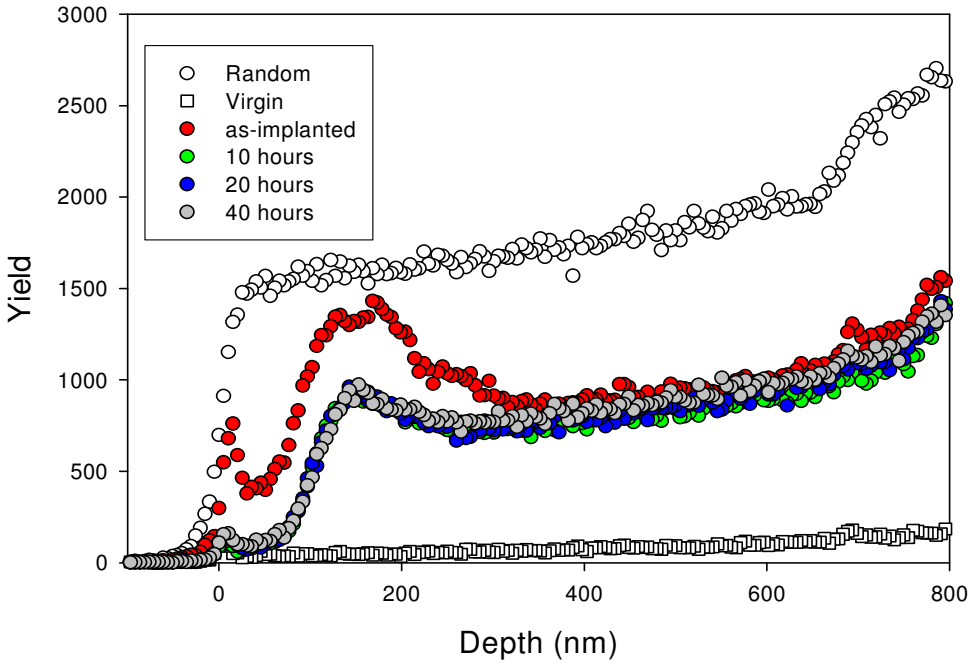

Figure 7-27: Random and aligned backscattering spectra from targets implanted at 350 °C with a fluence of 2×10^{16} $Ag^{+}cm^{-2}$ and subjected to isothermal annealing at 1300 °C for 10 hour cycles up to 40 hours.

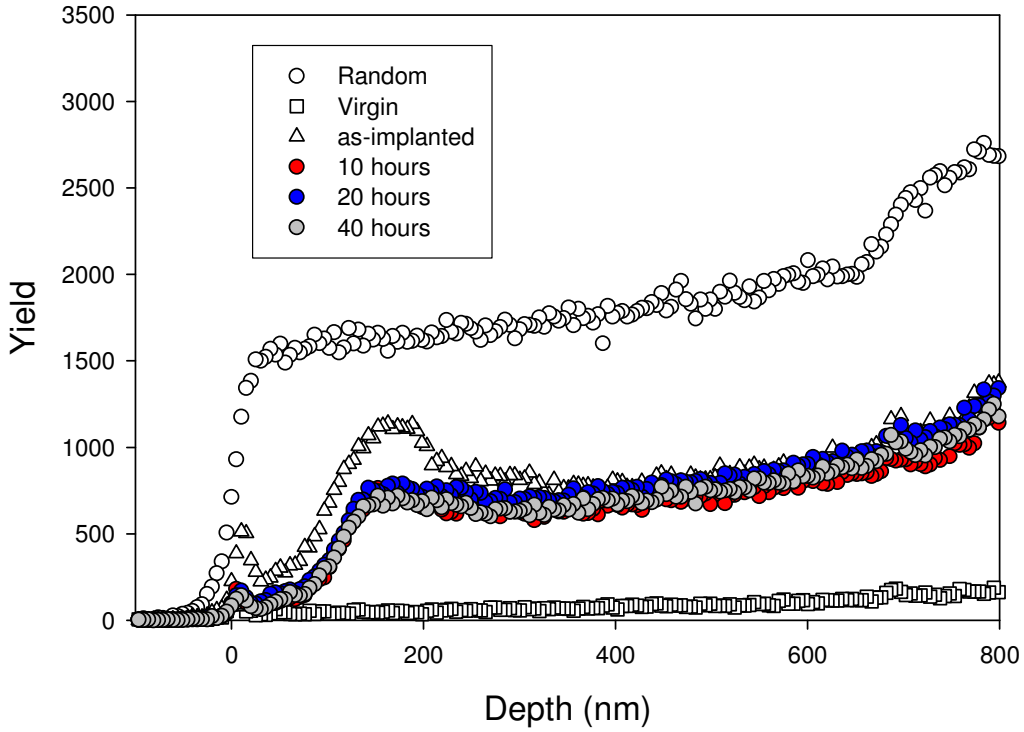

Figure 7-28: Random and aligned backscattering spectra from targets implanted at 600 °C with a fluence of 2×10^{16} $Ag^{+}cm^{-2}$ and subjected to isothermal annealing at 1350 °C for 10 hour cycles up to 40 hours.

Isothermal annealing of samples at 1300 °C for 10 hour cycles up to 40 hours (implanted at 350 °C and at 600 °C) caused some annealing of radiation damage created during implantation but a number of defects remained as shown in figure 7-27 and 7-28. Similar results were observed for isothermal annealing at 1300 °C and 1350 °C for 30 minutes, while isothermal annealing at 1500 °C of the same samples implanted at 600 °C for 30 minutes, 3 hours and 6 hours caused some defect removal as is clear from the reduction of the defect peaks around 180 nm; see figure 7-29. This defect annealing is greater during the first annealing cycle, i.e. 30 minutes (see the damage peak around 180 nm), but defects are still retained after annealing for 6 hours at 1500 °C. This is the result of defects annealing into dislocation networks (during the first annealing cycle) that are very difficult to anneal out during the first annealing cycle.

Our results are in disagreement with the results of Pacaud et al. [Pac96]. Pacaud et al. annealed the highly defective single crystalline of 6H-SiC at 500 °C, 950 °C and

1500 °C for 10 minutes. Their results showed that at 1500 °C all the defects were annealed out. The discrepancy in our results could be explained by the fact that in the case of Pacaud et al. the annealing of defects also took place from the low temperature annealing up to 1500 °C for a shorter period, while in our study it was only the isothermal annealing of the same samples at 1500 °C. Hence in our case the samples experienced the same thermal stresses during cooling to room temperature as in the experiments by Pacaud et al.

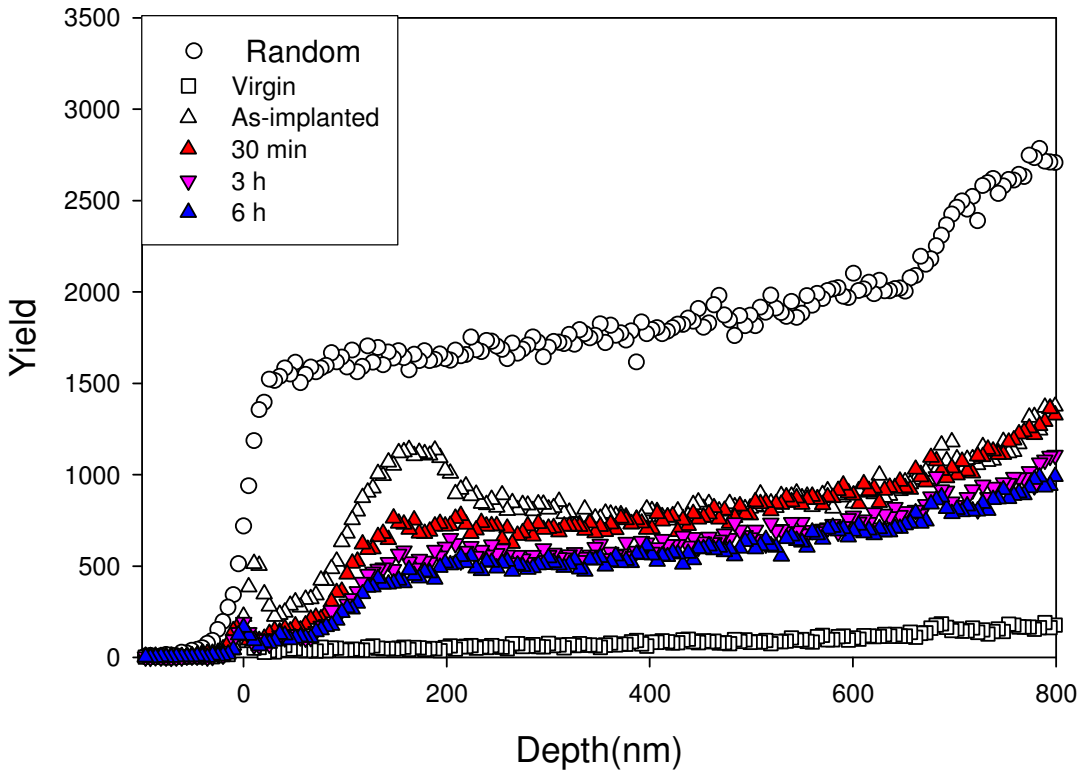

Figure 7-29: Random and aligned backscattering spectra from targets implanted at 600 °C with a fluence of 2×10^{16} $Ag^{+}cm^{-2}$ and submitted to isothermal annealing at 1500 °C for 30 minutes, 3 hours and 6 hours.

7.2.2.2 IMPLANTED LAYER DIFFUSION RESULTS

The typical depth profiles of silver implanted in 6H-SiC at room temperature, 350 °C and 600 °C were compared with TRIM 98 predictions and are shown in figure 7-30. Their moments are as follows: room temperature implantation (R_p = 109 nm σ = 39 nm, β = 2.98, γ = 0.15), 350 °C implantation (R_p = 102 nm, σ = 38.69 nm,

β = 2.83 and γ = 0.42), 600 ^{o}C implantation (R_p =102nm, σ = 40.2 nm, β = 3.03 and γ = 0.4) and TRIM98 (R_p =106 nm, σ = 26.78 nm, β = 2.78 nm and γ = 0.069).The projected range of silver implanted at room temperature is 2% deeper compared to those implanted at 350 ^{o}C and 600 ^{o}C. This is within experimental error and might also be due to the differences in stopping power between amorphous and crystalline SiC. The broader silver peaks in the measurements are due to the reasons discussed in section 7.2.1.2.

The depth profiles of silver implanted in 6H-SiC at 350 ^{o}C and at 600 ^{o}C after isothermal annealing at 1300 ^{o}C for 10 hour cycles up to 40 hours compared to the as-implanted profiles are displayed in figures 7-31 and 7-32. Their corresponding full widths at half maximum square $(FWHM)^2$'s are depicted in figure 7-33 and figure 7-34. From these results it is evident that no detectable diffusion of silver either into the bulk or towards the surface is taking place and that silver loss is almost zero for both samples at this annealing temperature. These results are in agreement with the results of Jiang et al. who found no diffusion of silver in crystalline SiC [Jia04].

The diffusion coefficient obtained from fitting the experimental data (for t_a =10 h to t_a= 40 h) to a straight line yields an upper limit of: $D_{6H} < 10^{-21}\ m^2s^{-1}$ at 1300 ^{o}C for 600 ^{o}C implanted samples. This result is of the same order of magnitude as the results of MacLean et al. [Mac06], who established an upper limit of: $D < 5\times10^{-21}\ m^2s^{-1}$ at 1500 ^{o}C even though our temperature is 200 ^{o}C less. This implies that our technique (RBS) exhibits a better depth resolution than the XPS used by MacLean et al. [Mac04]. Hence, if the diffusion coefficient is $D \sim 5\times10^{-21}\ m^2s^{-1}$ our RBS measurements should have detected it.

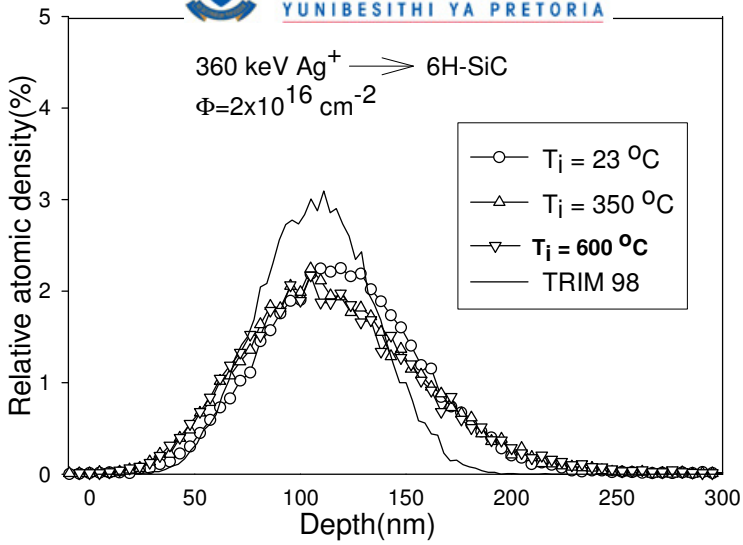

Figure 7-30: Depth profiles of silver implanted in 6H-SiC at room temperature, 350 °C and at 600 °C as compared with TRIM98 prediction.

Isothermal annealing of samples (implanted at 350 °C and 600 °C) at 1300 °C and 1350 °C for 30 minutes up to 120 minutes caused no diffusion of silver as can be observed from figure 7-35 and figure 7-36.

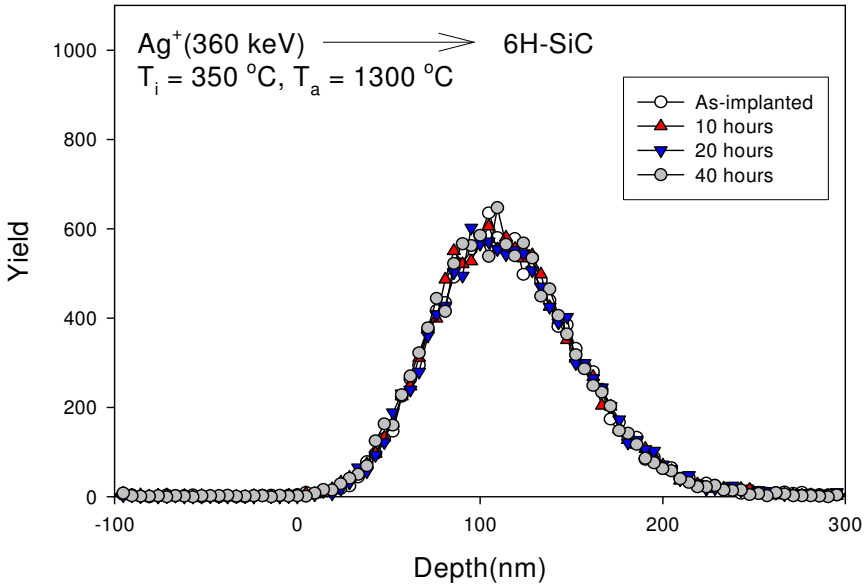

Figure 7-31: Depth profiles of silver implanted in 6H-SiC at 350 °C and isothermally annealed at 1300 °C for a 10 hour cycle up to 40 hours as compared with the as-implanted silver profile.

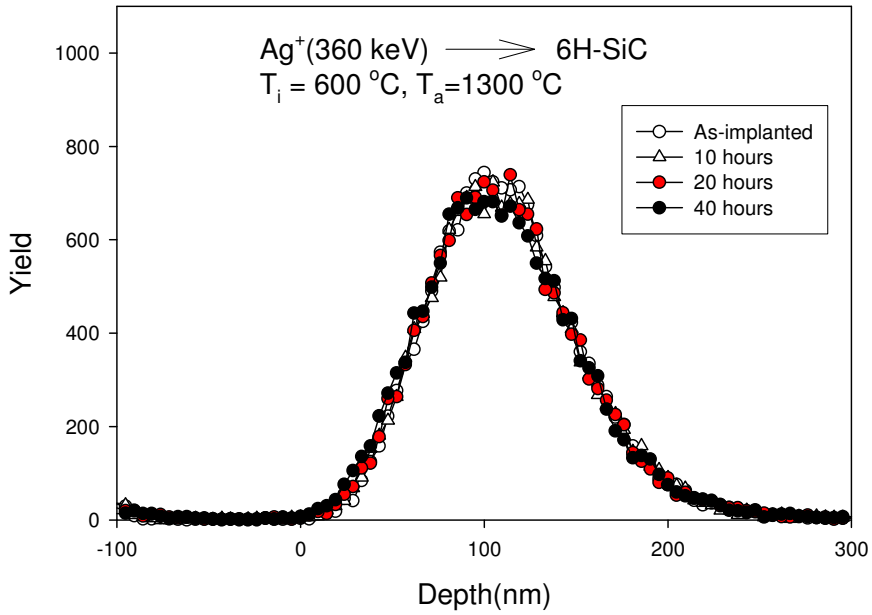

Figure 7-32: Depth profiles of silver implanted in 6H-SiC at 600 °C and isothermally annealed at 1300 °C for a 10 hour cycle up to 40 hours as compared with the as-implanted silver profile.

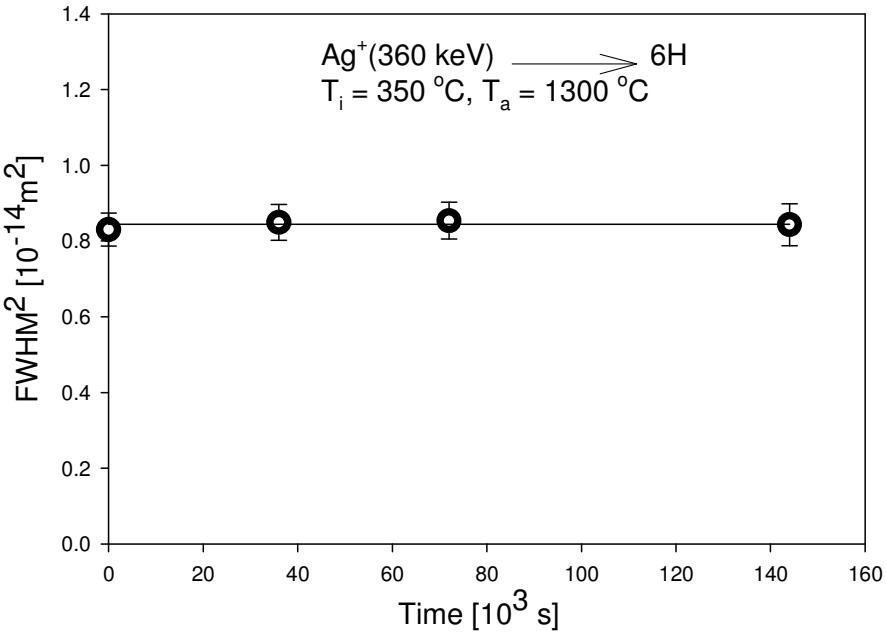

Figure 7-33: Square of the full width at half maximum (FWHM) of the silver profile in 6H-SiC as a function of isothermal annealing time at T_a=1300 °C for a 10 hour cycle up to 40 hours.

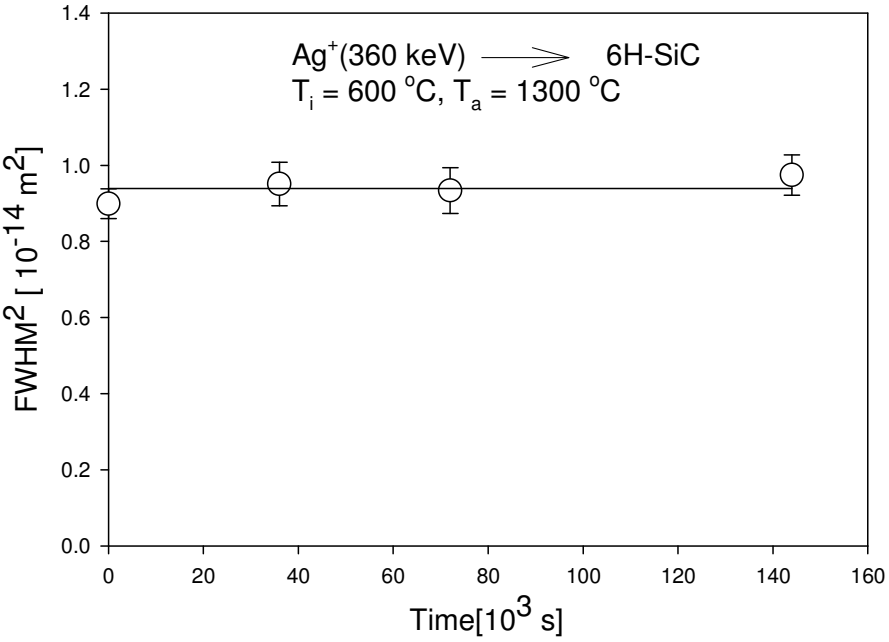

Figure 7-34: Square of the full width at half maximum (FWHM) of the silver profile in 6H-SiC as a function of isothermal annealing time at T_a=1300 °C for a 10 hour cycle up to 40 hours.

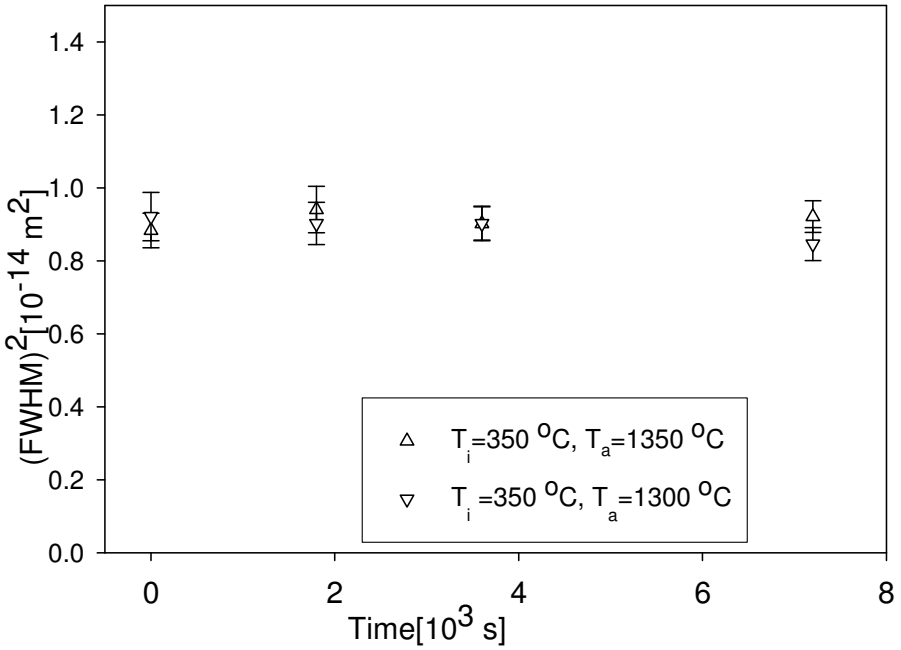

Figure 7-35: Square of the full width at half maximum $(FWHM)^2$ of the silver profiles implanted in 6H-SiC at 350 °C as a function of annealing time at Ta=1300 °C and Ta=1350 °C for a 30 minutes cycle up to 120 minutes.

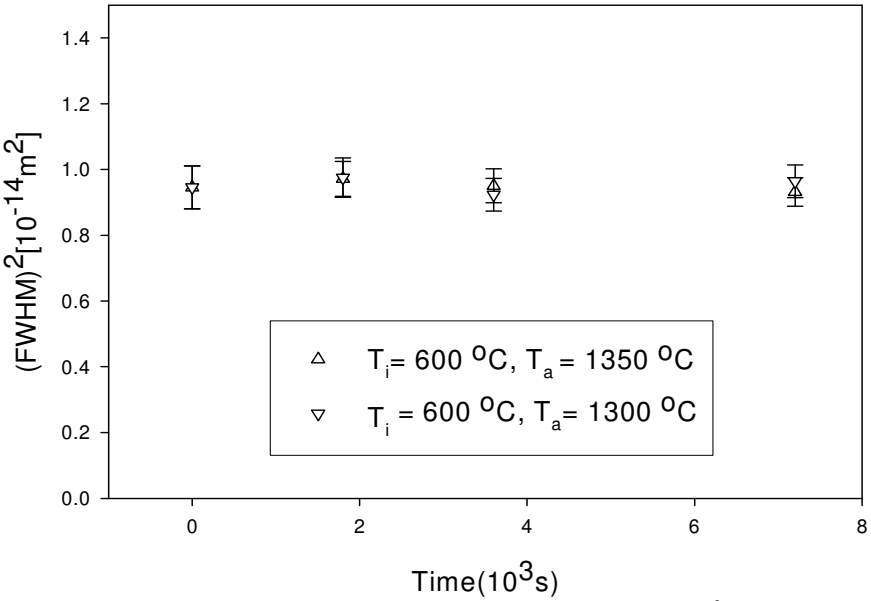

Figure 7-36: Square of the full width at half maximum $(FWHM)^2$ of the silver profiles implanted in 6H-SiC at 600 ^oC as a function of annealing time at T_a=1300 ^oC and T_a=1350 ^oC for a 30 minute cycle up to 120 minutes.

The immobility and negligible loss of silver at 1300 ^oC and 1350 ^oC in the samples implanted at 600 ^oC allowed further investigation of silver diffusion at temperatures higher than 1300 ^oC. Isothermal annealing of the sample (implanted at 600 ^oC) at 1500 ^oC was performed for different cycles. The results are illustrated in figures 7-37 to 7-40. RBS results showed that annealing at 1500 ^oC caused no broadening in the silver profiles, but the shift towards the surface was observed for annealing times as short as 30 minutes and was more pronounced at longer annealing times. SEM analyses of the SiC surface indicated the deterioration of the surface, which was probably due to the thermal etching of material during annealing [Cap98][Cap99]. This is evident from the formation of the steps in figure 7-40. These steps indicate that the etching rate is not uniform over the whole surface due to the damage created during implantation. Therefore, the shift of the silver peak towards the surface at 1500 ^oC is due to thermal etching (see figure 7-37 and figure 7-38). These results also explain the shift of the silver peak towards the surface observed at 1500 ^oC for 10 hours.

The slope of the silver peak position versus the annealing time (see figure 7-38) is steep during the first annealing cycle, indicating more thermal etching, but reduces as

the annealing cycle lengthens, indicating less thermal etching. This is because of the damage created during implantation, which results in weaker bonds in the SiC, thereby causing atoms to need less energy to escape. The amount of SiC etched was calculated by taking the difference between the as-implanted silver peak position and the silver peak position after annealing. For example, after annealing at 1500 ^{o}C for 6 hours, about 12 nm of SiC was etched away.

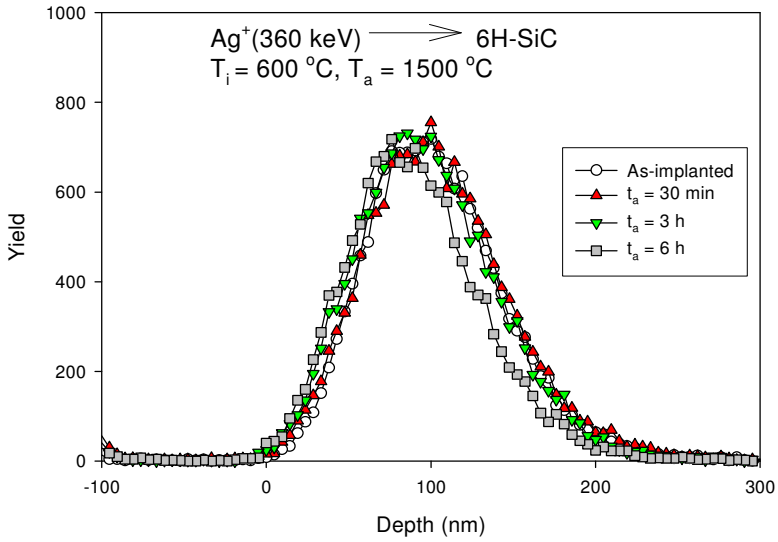

Figure 7-37: Depth profiles of silver implanted in 6H-SiC at 600 ^{o}C and isothermally annealed at 1500 ^{o}C from 30 minutes up to 6 hours compared with the as-implanted silver

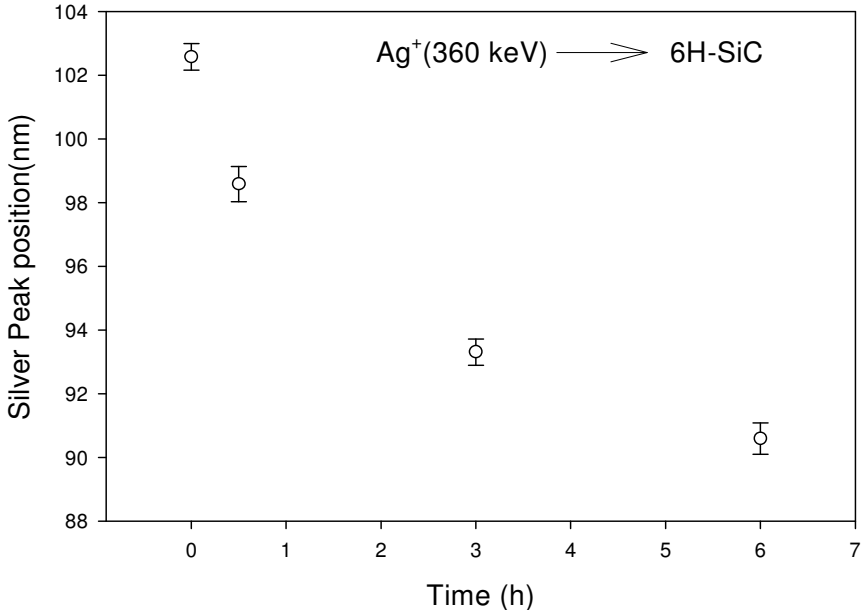

Figure 7-38: Peak position of silver implanted in 6H-SiC at 600 ^{o}C after isothermal annealing at 1500 ^{o}C up to 6 hours.

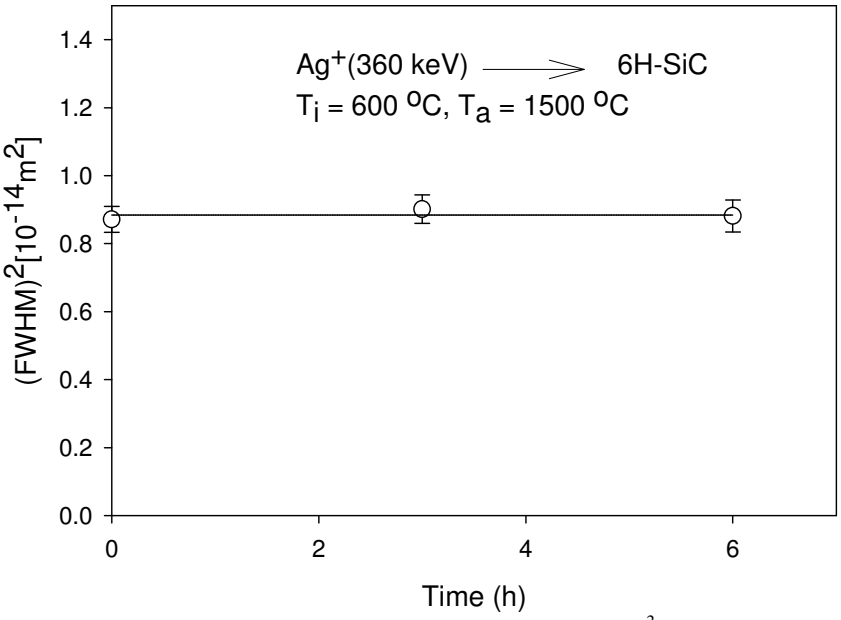

Figure 7-39: Square of the full width at half maximum square $(FWHM)^2$ of the silver profiles implanted in 6H-SiC at 600 °C as a function of isothermal annealing time up to 6 hours at Ta = 1500 °C.

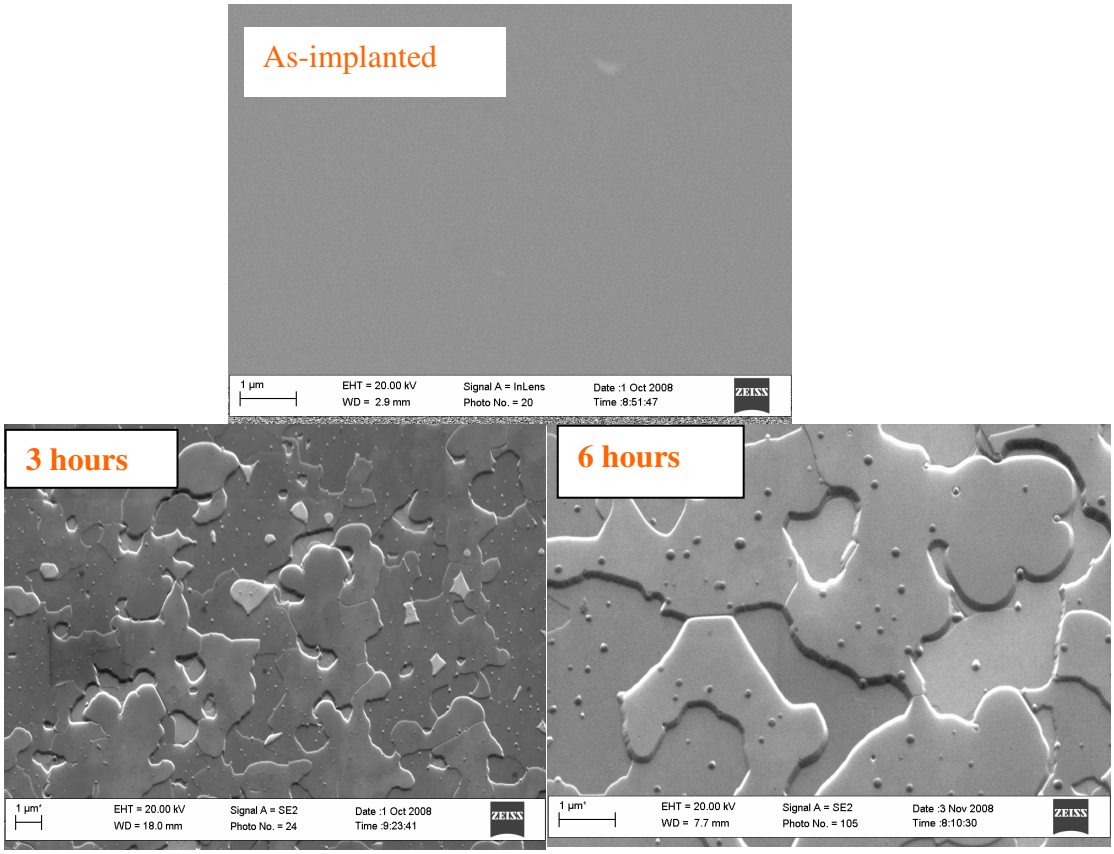

Figure 7-40: SEM images of 6H-SiC implanted at 600 °C after isothermal annealing at 1500 °C for different annealing cycles up to 6 hours.

7.2.2.3 EFFECT OF NEUTRON IRRADIATION

The effect of neutron irradiation was investigated on the samples implanted at higher temperatures (350 ^{o}C and 600 ^{o}C). This was performed because no diffusion was observed on these samples. Samples were irradiated by placing them in an experimental nuclear reactor (SAFARI-1) for 278 h, with a neutron flux of 1.46×10^{14} $cm^{-2}s^{-1}$; the reactor power was about 20 MW. The temperature of the samples during irradiation was approximately 300 ^{o}C. The samples were found to be radioactive after irradiation while the gamma ray spectrum was found to be that of ^{110m}Ag (see figure 7-41) with a half life of 253 days. ^{110m}Ag resulted from the implanted ^{109}Ag capturing neutrons during irradiation. Before analysing the samples with RBS, the maximum activity was estimated in each sample, by multiplying the maximum activity of ^{110m}Ag which is 4.7×10^{3} Ci/g by the mass of implanted silver. The mass of silver was calculated from the fluence of implanted ^{109}Ag ($2\times10^{16}cm^{-2}$) and the average area of the SiC samples (0.2 cm^{2}); it was found to be 7.2×10^{-7} g. Hence the maximum activity in one sample (A) was established as 3.4 mCi. To limit the exposure time during the RBS measurements, channelling was not performed on post irradiated samples.

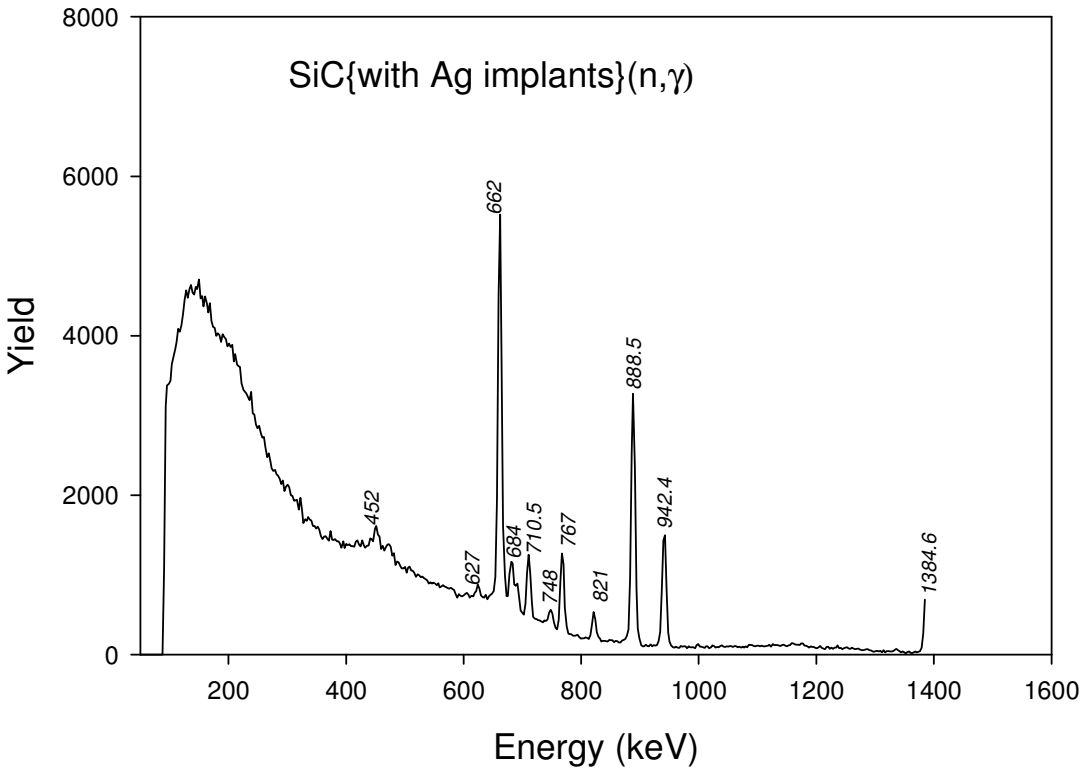

Figure 7-41: Gamma-rays measured on samples implanted with silver at 350 ^{o}C and 600 ^{o}C after neutron irradiation.

The silver profiles of the neutron irradiated sample which was implanted with Ag at 350 ^{o}C compared with the as-implanted silver profile are illustrated in figure 7-42. The as-implanted silver profile and the silver profile of the neutron irradiated profile are identical because RBS is unable to resolve the difference between ^{109}Ag and ^{110m}Ag. This is caused by the insufficient mass resolution of the RBS at high masses. The identical profiles indicate that neutron irradiation caused no diffusion of silver through SiC at room temperature. Similar results were observed in the samples implanted at 600 ^{o}C. No annealing was performed on these samples because any ^{110m}Ag release would contaminate the furnace which would endanger the personnel involved.

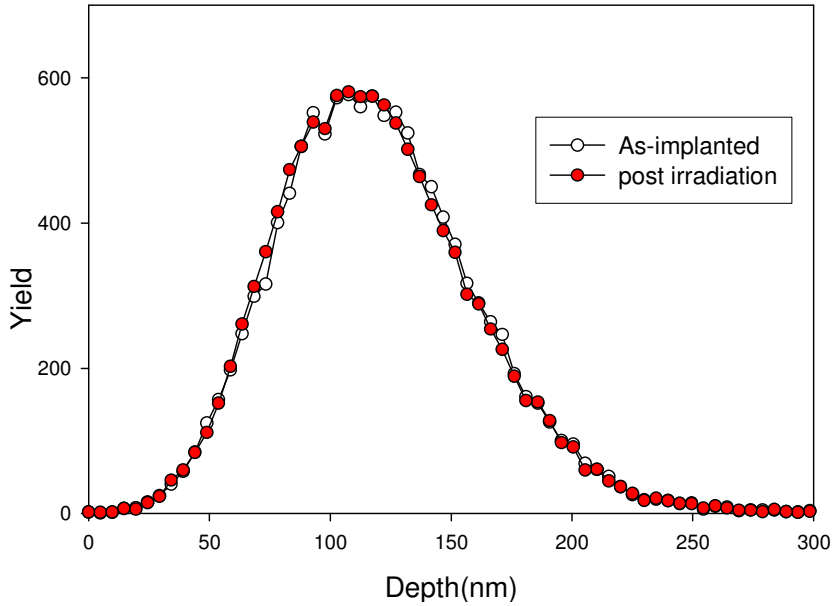

Figure 7-42: Silver depth profiles of the post irradiated SiC implanted (at 350 ^{o}C) compared with the as-implanted profiles.

7.3 REFERENCES

[Boh87] H. G. Bohn, J.M. Williams, C.J. McHargue, G.M. Begun, J. Mat. Res. **2** (1987) 106.

[Cap98] M. A. Capano, S. Ryu, M.R. Melloch, J. A. Jr. Cooper, M. R. Buss, J. Elec. Mat. **27** (1998) 370.

[Cap99] M. A. Capano, S. Ryu, J.A. Jr., Cooper, M. R. Melloch, K. Rottner, S. Karlsson, et al. J. Elec. Mat. **28** (1999) 214.

[Fel68] D.W. Feldmann, J. H. Parker, W. J. Choyke, L. Patrick, Phys. Rev. **170** (1968) 698.

[Fen99] Z. C. Feng, S. T. Chua, K. Tone, J. H. Zhao, Appl. Phys. Lett. 75 (199) 472

[Fri09] E. Friedland, J.B. Malherbe, N.G. van der Berg , T. Hlatshwayo, A.J. Botha, E. Wendler , W. Wesch, J.Nucl.Mat. **389** (2009) 326.

[Jia04] W. Jiang, W.J. Weber, V. Shutthanandan, L. Li, S. Thevuthasan, Nucl. Instr. and Meth. **219/220** (2004) 642.

[Mac06] H.J. MacLean, R.G. Ballinger, L.E. Kolaya, S.A. Simonson, N. Lewis, M.E. Hanson, J. Nucl. Mater. **357** (2006) 31.

[Nab77] H. Nabielek, P.E. Brown, P. Offermann, Nucl. Tech. **35** (1977) 483.

[Nak02] T. Nakamura, S. Matsumoto and M. Satoh, J. Cryst. Grow. **237-239** (2002) 1264.

[Pac96] Y. Pacaud, J. Stoemenos, G. Brauer, R.A. Yonkov, V. Heera, M. Voelskow, R. Kögler, W. Skorupa, Nucl. Instr. and Meth. **B120** (1996) 177.

[Rao03] M. V. Rao, Solid-State Electronics, **47** (2003) 213.

[Shu69] F.A. Shunk, *Constitution of Binary Alloys,* McGraw-Hill Company, New York (1969).

[Tes95] J. R. Tesmer, M. Nastasi, Handbook of Modern Ion Beam Materials Analysis, Mat. Res. Soc. Pittsburgh, Pennsylvania (1995)

[Wen98] E. Wendler, A. Heft, W. Wesch, Nucl. Instr. and Meth. **B141** (1998) 105.